

Online Adaptive Asymmetric Active Learning with Limited Budgets

Yifan Zhang, Peilin Zhao, Shuaicheng Niu, Qingyao Wu, Jiezhong Cao, Junzhou Huang, Mingkui Tan

Abstract—Online Active Learning (OAL) aims to manage unlabeled datastream by selectively querying the label of data. OAL is applicable to many real-world problems, such as anomaly detection in health-care and finance. In these problems, there are two key challenges: the query budget is often limited; the ratio between classes is highly imbalanced. In practice, it is quite difficult to handle imbalanced unlabeled datastream when only a limited budget of labels can be queried for training. To solve this, previous OAL studies adopt either asymmetric losses or queries (an isolated asymmetric strategy) to tackle the imbalance, and use first-order methods to optimize the cost-sensitive measure. However, the isolated strategy limits their performance in class imbalance, while first-order methods restrict their optimization performance. In this paper, we propose a novel Online Adaptive Asymmetric Active learning algorithm, based on a new asymmetric strategy (merging both asymmetric losses and queries strategies), and second-order optimization. We theoretically analyze its mistake bound and cost-sensitive metric bounds. Moreover, to better balance performance and efficiency, we enhance our algorithm via a sketching technique, which significantly accelerates the computational speed with quite slight performance degradation. Promising results demonstrate the effectiveness and efficiency of the proposed methods.

Index Terms—Active Learning; Online Learning; Class Imbalance; Budgeted Query; Sketching Learning.

1 INTRODUCTION

DU E to rapid growth of data and computational resources, machine learning addresses more and more practical problems, powering many aspects of modern society [1], [2], [3], [4], [5]. Nevertheless, many machine learning methods require the availability of sufficient off-line data before training, while those off-line samples are required to be i.i.d. [7], [8]. However, in many real-world applications, data comes in an online manner and the i.i.d. assumption may not hold. To address these limitations, online learning has emerged as a powerful tool [9], [10], [11], [12]. It makes no assumptions about the distribution of data and thus is data efficient and adaptable [7], [8].

Most existing online methods assume all samples are labeled, and ignore the labeling cost as well as the budget control problem. However, in many applications like medical diagnosis [2] and malicious URL detection [5], [13], the cost of annotation is often expensive. Hence, it is important to find out samples, which deserve to be labeled from data streams. To handle this task, online active learning (OAL) [14], [15] has emerged. It aims to train a well-performed model by selectively querying only a small number of labels for data streams. Many studies [4], [14], [15] have found that different query rules result in very different performance, which means that the query strategy is very important. Meanwhile, real-world companies usually expect to spend as few funds as possible for data annotation. In other words, we only have a limited budget for label querying. Given a limited budget, we have to select the most informative

samples to query so that they can help to train a well-performed model.

In addition, the class-imbalanced issue seriously affects algorithm performance in real-world applications, such as cancer diagnosis [2], financial credit monitoring [3] and network fraud detection [5]. Existing OAL methods usually train models using balanced *accuracy* or *mistake rate* as metrics. However, they cannot handle the imbalance issue well [10]. To solve this, researchers have proposed more informative metrics, such as the weighted *sum of sensitivity* and *specificity*, and the weighted *misclassification cost* [10].

Based on these metrics, a pioneering cost-sensitive online active learning algorithm (CSOAL) [5] was proposed to directly optimize asymmetrically cost-sensitive metrics for OAL. However, this method only adopts a symmetric query rule [14] and ignores the imbalance problem in data selection. Recently, online asymmetric active learning algorithm (OAAL) [4] discovered that using asymmetric query strategy helps to handle imbalanced data better. However, this method overlooks imbalance issues in the optimization process and tends to query more majority data due to the recommended parameter settings [4]. Hence, this method may lead to poor performance on minority data. In comparison, CSOAL is “asymmetric update plus symmetric query”, and OAAL is “symmetric update plus asymmetric query”. Both algorithms devise the asymmetric strategy from a different and isolated perspective, and thus may perform insufficiently in class-imbalance problems.

In addition, both algorithms only consider first-order information of data streams. However, when scales of different features vary significantly, these methods may converge slowly [9]. As a result, it is difficult for them to achieve a good solution when labeled data is quite limited. To deal with this issue, recent studies [16], [17] have found second-order information (*i.e.*, correlations between features) helps

- Y. Zhang, S. Niu, J. Cao, Q. Wu and M. Tan are with South China University of Technology, China. E-mail: {sezyifan, sensc, secaojiezhong}@mail.scut.edu.cn; {qyw, mingkuitan}@scut.edu.cn.
- P. Zhao and J. Huang are with Tencent AI Lab, China. Email: peilinzhao@hotmail.com; joehhuang@tencent.com.
- P. Zhao, S. Niu and Q. Wu are co-first authors; Corresponding to M. Tan.

to enhance online methods significantly.

In this paper, we propose a novel online adaptive asymmetric active (OA3) learning algorithm. By exploiting samples' second-order information, we develop a new asymmetric strategy, which considers both model optimization and label queries simultaneously. As a result, the proposed strategy addresses the class imbalance better and thus improves model performance. Moreover, we theoretically analyze the metric bounds of our proposed algorithm for the cases within budgets and over budgets, respectively.

Although enjoying the advantage of second-order information, our proposed algorithm may run slower than first-order methods, because the update of the correlation matrix is time-consuming. Therefore, it may be inappropriate for applications with quite high-dimensional datasets. To address this issue, we further propose two efficient variants of OA3 based on sketching techniques [20], [21], [22], [23].

We empirically evaluate the proposed methods on real-world datasets. Encouraging results confirm their effectiveness, efficiency and stability. We also examine the influences of algorithm parameters. Extensive results validate the algorithm characteristics.

The rest of this paper is organized as follows. We first present the problem formulation and the proposed algorithm in Section 2, followed by the theoretical analyses in Section 3. Next, we propose two efficient variants based on sketching techniques in Section 4. We empirically evaluate the proposed algorithms in Section 5, and conclude the paper in Section 6. Due to the page limitation, we put related work in Supplementary D.

2 SETUP AND ALGORITHM

In this section, we firstly introduce the problem formulation of the online active learning problem for budgeted imbalanced data. Next, we present the scheme of the proposed Online Adaptive Asymmetric Active (OA3) Learning algorithm. Lastly, relying on samples' second-order information, we propose a new asymmetric strategy, which consists of an asymmetric update rule and an asymmetric query rule.

2.1 Problem Formulation

Without loss of generality, we consider online binary classification under limited query budgets here. Streaming data comes in one by one $\{x_1, x_2, \dots, x_T\}$, where $x_t \in \mathbb{R}^d$ is a d -dimensional sample at time t , and T is the total quantity of samples. Note that all samples are unlabeled, and there is a limited query budget B for obtaining class label $y \in \{-1, 1\}$. The main task is to learn a well-performed online linear classifier $w \in \mathbb{R}^d$ with only limited labeled data. Moreover, the prediction of the classifier is $\hat{y} = \text{sign}(w^\top x)$.

Primarily, we define some notations: $\mathcal{M} = \{t \mid y_t \neq \text{sign}(w_t^\top x_t), \forall t \in [T]\}$ is the mistake index set, $\mathcal{M}_p = \{t \in \mathcal{M} \text{ and } y_t = +1\}$ is the positive set of mistake index and $\mathcal{M}_n = \{t \in \mathcal{M} \text{ and } y_t = -1\}$ is the negative one. In addition, we set $M = |\mathcal{M}|$, $M_p = |\mathcal{M}_p|$ and $M_n = |\mathcal{M}_n|$ to denote the number of total mistakes, positive mistakes and negative mistakes. Moreover, we denote the index sets of all positive samples and all negative samples by $\mathcal{I}_T^p = \{i \in [T] \mid y_i = +1\}$ and $\mathcal{I}_T^n = \{i \in [T] \mid y_i = -1\}$, where $T_p = |\mathcal{I}_T^p|$ and $T_n = |\mathcal{I}_T^n|$ denote the number of positive

samples and negative samples. For convenience, we assume the positive class as the minority class, i.e., $T_p \leq T_n$.

Traditional online algorithms often optimize *accuracy* or *mistake rate*, which treats samples from different class equally. These metrics, however, may be inappropriate for imbalanced data, since a trivial learner by simply classifying all data as negative can still achieve high accuracy. To address this issue, a more suitable metric is to measure the *sum* of weighted *sensitivity* and *specificity*, i.e.,

$$\text{sum} = \alpha_p \times \frac{T_p - M_p}{T_p} + \alpha_n \times \frac{T_n - M_n}{T_n}, \quad (1)$$

where $\alpha_p, \alpha_n \in [0, 1]$ are trade-off parameters between *sensitivity* and *specificity*, and $\alpha_p + \alpha_n = 1$. Note that when $\alpha_p = \alpha_n = 0.5$, the *sum* metric becomes the famous *balanced accuracy*. In general, the higher the *sum* value, the better the classification performance.

In addition, another metric is to measure the weighted misclassification *cost* suffered by the model, i.e.,

$$\text{cost} = c_p \times M_p + c_n \times M_n, \quad (2)$$

where $c_p, c_n \in [0, 1]$ denote the cost weights for positive and negative instances, and $c_p + c_n = 1$. The lower the *cost* value, the better the classification performance.

2.2 Algorithm Scheme

Inspired by the adaptive confidence weight technique [17], [26], we exploit samples' second order information. Assume that the online model satisfies a multivariate Gaussian distribution [17], i.e., $w \sim \mathcal{N}(\mu, \Sigma)$, where μ is the mean vector and Σ is the covariance matrix of distribution. Without loss of generality, the mean value μ_i represents the model's knowledge of the weight for feature i , while $\Sigma_{i,i}$ encodes the confidence of feature i . Generally, the smaller $\Sigma_{i,i}$, the more confidence the model has in the mean weight value μ_i . The covariance term $\Sigma_{i,j}$ keeps the correlations between weights i and j . Given a definite Gaussian distribution, it is more practical to simply use the mean vector $\mu = \mathbb{E}[w]$ to make predictions, i.e., $\hat{y} = \text{sign}(\mu^\top x)$ [16], [17], [19], where we denote $p = \mu^\top x$ as the predictive margin.

Formally, when receiving a new sample x_t in the t -th round, the learner needs to make a prediction \hat{y}_t and decide whether to query the true label y_t . If deciding to query, the learner will consume one unit budget, and then update the predictive vector μ_t based on the received painful loss from (x_t, y_t) . Otherwise, the model will ignore x_t . Note that the above process is performed within the limited query budget B . Once the available budget goes down to zero, the learner will stop querying true labels and thus stop updating. We summarize the algorithm scheme in Algo. 1.

Considering the class-imbalanced issue, there are two main challenges when designing this active algorithm.

1) **How to update** the model in an asymmetric way to obtain a well-performed model, which is described in Subsection 2.3.

2) **How to query** the most informative samples asymmetrically, which is described in Subsection 2.4.

Algorithm 1 Online Adaptive Asymmetric Active (OA3) Learning algorithm.

Input budget B ; learning rate η ; regular parameter γ .
Initialization $\mu_1 = 0, \Sigma_1 = I, B_1 = 0$.
1: **for** $t = 1 \rightarrow T$ **do**
2: Receive an example $x_t \in \mathbb{R}^d$;
3: Compute $p_t = \mu_t^\top x_t$;
4: Make the prediction $\hat{y}_t = \text{sign}(p_t)$;
5: Draw a variable $Z_t = \text{Query}(p_t) \in \{0, 1\}$;
6: **if** $Z_t = 1$ and $B_t < B$ **then**
7: Query the true label $y_t \in \{-1, +1\}$;
8: $B_{t+1} = B_t + 1$;
9: $\mu_{t+1}, \Sigma_{t+1} = \text{Update}(\mu_t, \Sigma_t; x_t, y_t)$.
10: **else**
11: $B_{t+1} = B_t, \mu_{t+1} = \mu_t, \Sigma_{t+1} = \Sigma_t$.
12: **end if**
13: **end for**

2.3 Adaptive Asymmetric Update Rule

To solve the class imbalance issue, our objective is either to maximize *sum* metric in Eq. (1) or to minimize *cost* metric in Eq. (2). Both objectives are equivalent to minimizing the following objective [10]:

$$\sum_{y_t=+1} \rho \mathbb{I}_{(y_t(\mu^\top x_t) < 0)} + \sum_{y_t=-1} \mathbb{I}_{(y_t(\mu^\top x_t) < 0)}, \quad (3)$$

where $\rho = \frac{\alpha_p T_n}{\alpha_n T_p}$ for maximizing *sum* metric and $\rho = \frac{c_p}{c_n}$ for minimizing *cost* metric, while $\mathbb{I}(\cdot)$ is the indicator function.

However, this objective is non-convex. To facilitate the optimization, we replace the indicator function with its convex variants, *i.e.*,

$$\ell_t(\mu) = (\rho \mathbb{I}_{(y=+1)} + \mathbb{I}_{(y=-1)}) \max\{0, 1 - y_t(\mu^\top x_t)\}. \quad (4)$$

At round t , when receiving a sample x_t and querying its label y_t , we can naturally exploit second-order information of data by minimizing the following objective [16], [17], *i.e.*,

$$D_{KL}(\mathcal{N}(\mu, \Sigma) || \mathcal{N}(\mu_t, \Sigma_t)) + \eta \ell_t(\mu) + \frac{1}{2\gamma} x_t^\top \Sigma x_t, \quad (5)$$

where η is the learning rate, γ is the regularized parameter and D_{KL} denotes the Kullback-divergence, *i.e.*,

$$D_{KL}(\mathcal{N}(\mu, \Sigma) || \mathcal{N}(\mu_t, \Sigma_t)) = \frac{1}{2} \log \left(\frac{\det \Sigma_t}{\det \Sigma} \right) + \frac{1}{2} \text{Tr}(\Sigma_t^{-1} \Sigma) + \frac{1}{2} \|\mu_t - \mu\|_{\Sigma_t^{-1}}^2 - \frac{d}{2}.$$

Specifically, the objective of Eq. (5) helps to reach the trade-off between distribution divergence (first term), loss function (second term) and model confidence (third term). In other words, the objective tends to make the least adjustment to minimize the painful loss and optimize the model confidence. However, this optimization does not have closed-form solution. To address this issue, we replace the loss $\ell(\mu)$ with its first order Taylor expansion $\ell(\mu_t) + g_t^\top (\mu - \mu_t)$, where $g_t = \partial \ell_t(\mu_t)$. We then obtain the final optimization objective by removing constant terms, *i.e.*,

$$f_t(\mu, \Sigma) = D_{KL}(\mathcal{N}(\mu, \Sigma) || \mathcal{N}(\mu_t, \Sigma_t)) + \eta g_t^\top \mu + \frac{1}{2\gamma} x_t^\top \Sigma x_t, \quad (6)$$

which is much easier to be solved. We solve this optimization problem in two steps, iteratively:

- Update the mean parameter:

$$\mu_{t+1} = \arg \min_{\mu} f_t(\mu, \Sigma);$$

- If $\ell_t(\mu_t) \neq 0$, update the covariance matrix:

$$\Sigma_{t+1} = \arg \min_{\Sigma} f_t(\mu, \Sigma).$$

For the first step, setting the derivative $\partial_{\mu} f_t(\mu_{t+1}, \Sigma)$ to zero will give:

$$\Sigma_t^{-1}(\mu_{t+1} - \mu_t) + \eta g_t = 0 \implies \mu_{t+1} = \mu_t - \eta \Sigma_t g_t.$$

Second, setting derivative $\partial_{\Sigma} f_t(\mu, \Sigma_{t+1})$ to zero gives:

$$-\Sigma_{t+1}^{-1} + \Sigma_t^{-1} + \frac{x_t x_t^\top}{\gamma} = 0 \implies \Sigma_{t+1}^{-1} = \Sigma_t^{-1} + \frac{x_t x_t^\top}{\gamma}. \quad (7)$$

Based on the Woodbury identity [27], we have:

$$\Sigma_{t+1} = \Sigma_t - \frac{\Sigma_t x_t x_t^\top \Sigma_t}{\gamma + x_t^\top \Sigma_t x_t}. \quad (8)$$

Apparently, the update of the predictive vector relies on the confidence Σ . Thus, we update the mean vector μ_t based on the updated covariance matrix Σ_{t+1} , which will be more accurate and aggressive [16], [19], *i.e.*,

$$\mu_{t+1} = \mu_t - \eta \Sigma_{t+1} g_t. \quad (9)$$

We summarize the adaptive asymmetric update strategy in Algo. 2.

Algorithm 2 Adaptive Asymmetric Update Strategy: **Update**($\mu_t, \Sigma_t; x_t, y_t$).

Input $\rho = \frac{\alpha_p T_n}{\alpha_n T_p}$ for *sum* or $\rho = \frac{c_p}{c_n}$ for *cost*;

- 1: Receive a sample (x_t, y_t) ;
 - 2: Compute the loss $\ell_t(\mu_t)$, based on Equation (4);
 - 3: **if** $\ell_t(\mu_t) > 0$ **then**
4: $\Sigma_{t+1} = \Sigma_t - \frac{\Sigma_t x_t x_t^\top \Sigma_t}{\gamma + x_t^\top \Sigma_t x_t}$;
5: $\mu_{t+1} = \mu_t - \eta \Sigma_{t+1} g_t$, where $g_t = \partial \ell_t(\mu_t)$.
6: **else**
7: $\mu_{t+1} = \mu_t, \Sigma_{t+1} = \Sigma_t$.
8: **end if**
9: **Return** μ_{t+1}, Σ_{t+1} .
-

Time Complexity Analysis. Time complexities of updating for μ and Σ are both $\mathcal{O}(Td^2)$, so the overall time complexity of this update strategy is $\mathcal{O}(Td^2)$, where d is the dimension of data. Nevertheless, the update efficiency of OA3 is slower than first-order algorithms ($\mathcal{O}(Td)$), especially when handling high-dimensional datasets. To promote the efficiency, we propose a **diagonal version** of the update strategy (the pseudo-code is put in Supplementary B.1), which accelerates the efficiency to $\mathcal{O}(Td)$. Specifically, in this variant, only the diagonal entries of Σ are maintained and updated in each round.

Remark. We employ the adaptive asymmetric update rule for OA3 to pursue high performance with faster convergence. Nevertheless, it is not the only choice. Other classic techniques can also be used, *e.g.*, online gradient descent [10] and online margin-based strategies [9], [11].

2.4 Asymmetric Query Strategy

In a pioneering study [14], one classic sampling method was proposed to query labels based on a Bernoulli random variable $Z_t \in \{0, 1\}$. That is, querying the label for a given instance only when $Z_t = 1$. To be specific, the probability of sampling Z_t depends on the absolute value of the predictive margin $|p_t|$, *i.e.*,

$$\Pr(Z_t = 1) = \frac{\delta}{\delta + |p_t|},$$

where $\delta > 0$ is the query bias. In this equation, when the absolute predictive margin $|p_t|$ is low, the probability to query the label of sample x_t is relatively high. This is because when the sample's prediction is close to the classification hyperplane (small $|p_t|$), the sample is difficult to be classified and hence is more valuable to be queried (high $\Pr(Z_t = 1)$).

However, this query rule ignores the imbalance of data and treats predictions of two imbalanced classes equally. To address this limitation, inspired by recent work [4], we employ an asymmetric strategy to query labels, *i.e.*,

$$\Pr(Z_t = 1) = \begin{cases} \frac{\delta_+}{\delta_+ + |p_t|}, & \text{if } p_t \geq 0; \\ \frac{\delta_-}{\delta_- + |p_t|}, & \text{if } p_t < 0; \end{cases}$$

where $\delta_+ > 0$ and $\delta_- > 0$ denote query biases for positive and negative predictions, respectively.

However, this asymmetric query strategy heavily depends on the absolute value of margin p_t , which is directly calculated by the model μ_t . As a result, the query decisions may be inaccurate when μ_t is not precise enough [32].

To address this issue, we use samples' second order information to enhance the query strategy and improve the robustness of the query judgement. We first define the variance of a model on the sample x_t as $v_t = x_t^\top \Sigma_t x_t$. It represents the familiarity of the model with the current sample through previous experience. Based on v_t , we then define the query confidence:

$$c_t = -\frac{1}{2} \frac{\eta \rho_{max}}{\frac{1}{v_t} + \frac{1}{\gamma}}, \quad (10)$$

where $\rho_{max} = \max\{1, \rho\}$. We highlight that this equation is helpful for the theoretical analysis. Moreover, the confidence c_t directly depends on the variance v_t . Based on this equation, when the model has been well trained on some instances similar to the current sample x_t (*i.e.*, low variance v_t), the model would be confident of this sample (*i.e.*, large confidence c_t).

Based on the predictive margin and the confidence, we obtain the final query parameter:

$$q_t = |p_t| + c_t. \quad (11)$$

Moreover, both the learning rate η and regularized parameter γ in Eq. (10) can be understood as trade-off factors in Eq. (11).

Relying on above analyses, we propose an improved asymmetric query strategy:

$$\Pr(Z_t = 1) = \begin{cases} \frac{\delta_+}{\delta_+ + q_t}, & \text{if } p_t \geq 0; \\ \frac{\delta_-}{\delta_- + q_t}, & \text{if } p_t < 0. \end{cases}$$

To be specific, when $q_t > 0$, the query decision of the model is very confident, so we directly draw a Bernoulli variable based on this equation. If $q_t \leq 0$, the query decision is unconfident of the current sample, so we decide to query the true label whatever the value of p_t , *i.e.*, obtaining $Z_t = 1$ by setting $q_t = 0$ (see the above equation).

We summarize the proposed asymmetric query strategy in Algo. 3.

Algorithm 3 Asymmetric Query Strategy: Query(p_t).

Input $\rho_{max} = \max\{1, \rho\}$; query bias (δ_+, δ_-) for positive and negative predictions.

- 1: Compute the variance $v_t = x_t^\top \Sigma_t x_t$;
 - 2: Compute the query parameter $q_t = |p_t| - \frac{1}{2} \frac{\eta \rho_{max}}{\frac{1}{v_t} + \frac{1}{\gamma}}$;
 - 3: **if** $q_t \leq 0$ **then**
 - 4: Set $q_t = 0$;
 - 5: **end if**
 - 6: **if** $p_t \geq 0$ **then**
 - 7: $p_t^+ = \frac{\delta_+}{\delta_+ + q_t}$;
 - 8: Draw a Bernoulli variable $Z_t \in \{0, 1\}$ with p_t^+ ;
 - 9: **else**
 - 10: $p_t^- = \frac{\delta_-}{\delta_- + q_t}$;
 - 11: Draw a Bernoulli variable $Z_t \in \{0, 1\}$ with p_t^- ;
 - 12: **end if**
 - 13: **Return** Z_t .
-

We can obtain the expected number of queried samples without budget limitations as follows.

Proposition 1. Based on the proposed asymmetric query strategy, the expected number of requested samples without a budget is:

$$\sum \mathbb{I}_{(q_t \leq 0)} + \sum_{\substack{q_t > 0 \\ p_t \geq 0}} \frac{\delta_+}{\delta_+ + q_t} + \sum_{\substack{q_t > 0 \\ p_t < 0}} \frac{\delta_-}{\delta_- + q_t}.$$

3 THEORETICAL ANALYSIS

We next analyze the proposed algorithm in terms of its mistake bound and two cost-sensitive metric bounds, for the cases within budgets and over budgets, respectively. Before that, we first show a lemma, which facilitates the analysis within budgets. Due to the page limitation, all proofs are put in Supplementary A.

For convenience, we introduce the following notations:

$$M_t = \mathbb{I}_{(y_t \neq y_t)}, \quad \rho = \frac{\alpha_p T_n}{\alpha_n T_p} \text{ or } \frac{c_p}{c_n},$$

$$\rho_t = \rho \mathbb{I}_{(y_t = +1)} + \mathbb{I}_{(y_t = -1)}, \quad \rho_{max} = \max\{1, \rho\}, \quad \rho_{min} = \min\{1, \rho\}.$$

Lemma 1. Let $(x_1, y_1), \dots, (x_T, y_T)$ be a sequence of input samples, where $x_t \in \mathbb{R}^d$ and $y_t \in \{-1, +1\}$ for all t . Let T_B be the round that runs out of the budgets, *i.e.*, $B_{T_B+1} = B$. For any $\mu \in \mathbb{R}^d$ and any $\delta > 0$, OA3 algorithm satisfies:

$$\sum_{t=1}^{T_B} M_t Z_t (\delta + q_t) \leq \frac{\delta}{\rho_{min}} \sum_{t=1}^{T_B} \ell_t(\mu) + \frac{1}{\eta \rho_{min}} \text{Tr}(\Sigma_{T_B+1}^{-1}) \times [M(\mu) + (1 - \delta)^2 \|\mu\|^2],$$

where $M(\mu) = \max_t \|\mu_t - \mu\|^2$.

Based on Lemma 1, we obtain the following three theorems for the case **within budgets**.

Theorem 1. Let $(x_1, y_1), \dots, (x_T, y_T)$ be a sequence of input samples, where $x_t \in \mathbb{R}^d$ and $y_t \in \{-1, +1\}$ for all t . Let T_B be the round that runs out of the budgets, i.e., $B_{T_B+1} = B$. For any $\mu \in \mathbb{R}^d$, the expected mistake number of OA3 within budgets is bounded by:

$$\begin{aligned} \mathbb{E} \left[\sum_{t=1}^{T_B} M_t \right] &= \mathbb{E} \left[\sum_{\substack{t=1 \\ y_t=+1}}^{T_B} M_t + \sum_{\substack{t=1 \\ y_t=-1}}^{T_B} M_t \right] \\ &\leq \frac{1}{\rho_{\min}} \left[\sum_{t=1}^{T_B} \ell_t(\mu) + \frac{1}{\eta} D(\mu) \text{Tr}(\Sigma_{T_B+1}^{-1}) \right], \end{aligned}$$

where $D(\mu) = \max \left\{ \frac{M(\mu) + (1-\delta_+)^2 \|\mu\|^2}{\delta_+}, \frac{M(\mu) + (1-\delta_-)^2 \|\mu\|^2}{\delta_-} \right\}$.

This mistake bound helps to analyze the weighted *sum* performance under limited budgets.

Theorem 2. Under the same condition in Theorem 1, by setting $\rho = \frac{\alpha_p T_n}{\alpha_n T_p}$, the proposed OA3 within budgets satisfies for any $\mu \in \mathbb{R}^d$:

$$\mathbb{E} \left[\text{sum} \right] \geq 1 - \frac{\alpha_n \rho_{\max}}{T_n \rho_{\min}} \left[\sum_{t=1}^{T_B} \ell_t(\mu) + \frac{1}{\eta} D(\mu) \text{Tr}(\Sigma_{T_B+1}^{-1}) \right].$$

Remark. By setting $\alpha_p = \alpha_n = 0.5$, we can easily obtain the bound of the balanced accuracy.

Note that α_n cannot be set to zero, because $\rho = \frac{\alpha_p T_n}{\alpha_n T_p}$. One restriction is that we could not acquire $\frac{T_n}{T_p}$ in advance in real-world tasks. To overcome this limitation, we can choose *cost* metric as an alternative, where $\rho = \frac{c_p}{c_n}$. In this sense, engineers need not worry $\frac{T_n}{T_p}$ any more. Next, we bound the cumulative *cost* performance under limited budgets.

Theorem 3. Under the same condition in Theorem 1, by setting $\rho = \frac{c_p}{c_n}$, the proposed OA3 within budgets satisfies for any $\mu \in \mathbb{R}^d$:

$$\mathbb{E} \left[\text{cost} \right] \leq \frac{c_n \rho_{\max}}{\rho_{\min}} \left[\sum_{t=1}^{T_B} \ell_t(\mu) + \frac{1}{\eta} D(\mu) \text{Tr}(\Sigma_{T_B+1}^{-1}) \right].$$

Note that c_n cannot be set to zero, since $\rho = \frac{c_p}{c_n}$.

By now, we have analyzed OA3 algorithm within budgets. Next, we analyze OA3 for the case **over budgets**.

Theorem 4. Let $(x_1, y_1), \dots, (x_T, y_T)$ be a sample stream, where $x_t \in \mathbb{R}^d$ and $y_t \in \{-1, +1\}$. Let T_B be the round that uses up the budgets, i.e., $B_{T_B+1} = B$. For any $\mu \in \mathbb{R}^d$, the expected mistakes of OA3 over budgets is bounded by:

$$\mathbb{E} \left[\sum_{T_B+1}^T M_t \right] \leq \sum_{T_B+1}^T \left[\frac{\ell_t(\mu)}{\rho_{\min}} + y_t x_t^\top \mu_{T_B+1} \right],$$

where μ_{T_B+1} is the predictive vector of model, trained by all the previous queried samples.

Now, we bound the weighted *sum* and misclassification *cost* after running out of budgets.

Theorem 5. Under the same condition in Theorem 4, by setting $\rho = \frac{\alpha_p T_n}{\alpha_n T_p}$, the sum performance of OA3 over budgets satisfies for any $\mu \in \mathbb{R}^d$:

$$\mathbb{E} \left[\text{sum} \right] \geq 1 - \frac{\alpha_n \rho_{\max}}{T_n} \sum_{T_B+1}^T \left[\frac{\ell_t(\mu)}{\rho_{\min}} + y_t x_t^\top \mu_{T_B+1} \right].$$

Theorem 6. Under the same condition in Theorem 4, by setting $\rho = \frac{c_p}{c_n}$, the misclassification cost of OA3 over budgets satisfies for any $\mu \in \mathbb{R}^d$:

$$\mathbb{E} \left[\text{cost} \right] \leq c_n \rho_{\max} \sum_{T_B+1}^T \left[\frac{\ell_t(\mu)}{\rho_{\min}} + y_t x_t^\top \mu_{T_B+1} \right].$$

4 ENHANCED ALGORITHM WITH SKETCHING

As mentioned above, OA3 requires $\mathcal{O}(Td^2)$ time complexity. The diagonal version accelerates the time complexity to $\mathcal{O}(Td)$. However, it cannot enjoy the correlation information between different dimensions of samples. When instances have low *effective rank*, the regret bound of OA3_{diag} may be much worse than its full-matrix version, because it lacks enough dependence on data dimensionality [22]. Unfortunately, many real-world high-dimensional datasets have such low-rank settings with abundant correlations among features. For these datasets, it is more appropriate to consider the complete feature correlations (i.e., adopting its full-matrix version) and also the efficiency issue.

To better balance performance and efficiency, we propose two efficient variants of our OA3 algorithm, which use the sketch method to approximate the inverse of the covariance matrix. Specifically, we first propose Sketched Online Adaptive Asymmetric Active (SOA3) Learning algorithm in Subsection 4.1 and then present its sparse version (SSAO3) in Subsection 4.2.

4.1 Sketched Algorithm

By exploiting the Oja's sketch method, we propose a SAO3 algorithm [20], [28] to accelerate our algorithm when facing high-dimensional datasets.

The Oja's sketch [29] is a method to compute the dominant eigenvalues and corresponding eigenvectors of a $n \times n$ matrix A . In Oja's method, matrix A has the following property: A itself is unknown but there is an available sequence $A_k, k=1, 2, \dots$ with $E\{A_k\} = A$ for all k . In our proposed OA3 algorithm, the computation of inverse covariance matrix Σ^{-1} in Eq. 7 can be transformed into this formula. Thus, the Oja's sketch method can be introduced to our OA3 algorithm.

In SOA3, we exploit Oja's sketch to search m carefully selective directions and use them to approximate our second-order inverse covariance matrix. Here, m is a small constant and called as the sketch size. According to Eqs. (8-9), we know the updating rule of the model weight μ :

$$\mu_{t+1} = \mu_t - \eta \Sigma_{t+1} g_t,$$

and the incremental formula of the covariance matrix:

$$\Sigma_{t+1}^{-1} = \Sigma_t^{-1} + \frac{x_t x_t^\top}{\gamma},$$

which can be expressed in another way:

$$\Sigma_{t+1}^{-1} = I_d + \sum_{i=1}^t \frac{x_i x_i^\top}{\gamma}, \quad (12)$$

where d is the dimensionality of instance. Let $X \in \mathbb{R}^{t \times d}$ be a matrix, whose t -th row is \hat{x}_t^\top , where we define $\hat{x}_t = \frac{x_t}{\sqrt{\gamma}}$ as the *to-sketch vector*. Hence, Eq. (12) can be written as:

$$\Sigma_{t+1}^{-1} = I_d + X_t^\top X_t.$$

The idea of sketching is to maintain a sketch matrix $S_t \in \mathbb{R}^{m \times d}$, where $m \ll d$. When m is chosen so that $S_t^\top S_t$ can approximate $X_t^\top X_t$ well, the Eq. (12) can be redefined as:

$$\Sigma_{t+1}^{-1} = I_d + S_t^\top S_t.$$

By Woodbury identity [27], we have:

$$\Sigma_{t+1} = I_d - S_t^\top H_t S_t, \quad (13)$$

where $H_t = (I_m + S_t S_t^\top)^{-1} \in \mathbb{R}^{m \times m}$. We rewrite the updating rule of μ :

$$\mu_{t+1} = \mu_t - \eta(g_t - S_t^\top H_t S_t g_t). \quad (14)$$

We summarize SOA3 in Algo. 4.

Algorithm 4 Sketched Online Adaptive Asymmetric Active (SOA3) Learning algorithm.

Input budget B ; learning rate η ; regularized parameter γ ; sketch size m ; bias $\rho = \frac{\alpha_p * T_n}{\alpha_n * T_p}$ for *sum* and $\rho = \frac{c_p}{c_n}$ for *cost*.

Initialization $\mu_1=0, B_1=0$.

Initialization $(S_0, H_0) \leftarrow \text{SketchInit}(m)$; (See Algo. 5)

```

1: for  $t = 1 \rightarrow T$  do
2:   Receive sample  $x_t$ ;
3:   Compute  $p_t = \mu_t^\top x_t$ ;
4:   Make the prediction  $\hat{y}_t = \text{sign}(p_t)$ ;
5:   Draw  $Z_t = \text{SketchQuery}(p_t) \in \{0, 1\}$ ; (See Algo. 6)
6:   if  $Z_t = 1$  and  $B_t < B$  then
7:     Query the true label  $y_t \in \{-1, +1\}$ ,  $B_{t+1} = B_t + 1$ ;
8:     Compute the loss  $\ell_t(\mu_t)$ , based on Equation (4);
9:     Compute the  $t$ -sketch vector  $\hat{x}_t = \frac{x_t}{\sqrt{\gamma}}$ ;
10:     $(S_t, H_t) \leftarrow \text{SketchUpdate}(\hat{x})$ ; (See Algo. 5)
11:    if  $\ell_t(\mu_t) > 0$  then
12:       $\mu_{t+1} = \mu_t - \eta(g_t - S_t^\top H_t S_t g_t)$ , where  $g_t = \partial_{\mu} \ell_t(\mu_t)$ ;
13:    else
14:       $\mu_{t+1} = \mu_t$ ;
15:    end if
16:  else
17:     $\mu_{t+1} = \mu_t$ ,  $B_{t+1} = B_t$ ,  $S_t = S_{t-1}$ ,  $H_t = H_{t-1}$ .
18:  end if
19: end for

```

We next discuss how to maintain matrices S_t and H_t efficiently via sketching technique. Specifically, with *to-sketch vector* x_t as input, the eigenvalues and eigenvectors of sequential data are computed by online gradient descent.

At round t , let the diagonal matrix $\Lambda_t \in \mathbb{R}^{m \times m}$ contain m estimated eigenvalues and let $V_t \in \mathbb{R}^{m \times d}$ denote the corresponding eigenvectors. The update rules of Λ_t and V_t using Oja's algorithm are defined as:

$$\Lambda_t = (I_m - \Gamma_t) \Lambda_{t-1} + \Gamma_t \text{diag}\{V_{t-1} \hat{x}_t\}^2, \quad (15)$$

$$V_t \xleftarrow{\text{orth}} V_{t-1} + \Gamma_t V_{t-1} \hat{x}_t \hat{x}_t^\top, \quad (16)$$

where $\Gamma_t \in \mathbb{R}^{m \times m}$ is a diagonal matrix whose diagonal elements are learning rates. In this paper, we set $\Gamma_t = \frac{1}{t} I_m$.

The " $\xleftarrow{\text{orth}}$ " operator represents an orthonormalizing step¹. Hence, the sketch matrices can be obtained by:

$$S_t = (t\Lambda)^{\frac{1}{2}} V_t, \quad (17)$$

$$H_t = \text{diag}\left\{\frac{1}{1+t\Lambda_{1,1}}, \dots, \frac{1}{1+t\Lambda_{m,m}}\right\}.$$

The rows of V_t are always orthonormal and thus H_t is an efficiently maintainable diagonal matrix. We summarize the Oja's sketching technique in Algo. 5.

Algorithm 5 Oja's Sketch for SOA3

Input m, \hat{x} and stepsize matrix Γ_t .

Internal State t, Λ, V and H .

SketchInit(m)

- 1: Set $t = 0, S = 0_{m \times d}, H = I_m, \Lambda = 0_{m \times m}$ and V to any $m \times d$ matrix with orthonormal rows;
- 2: Return (S, H) .

SketchUpdate(\hat{x})

- 1: Update $t \leftarrow t + 1$;
 - 2: Update $\Lambda = (I_m - \Gamma_t) \Lambda + \Gamma_t \text{diag}\{V \hat{x}\}^2$;
 - 3: Update $V \xleftarrow{\text{orth}} V + \Gamma_t V \hat{x} \hat{x}^\top$;
 - 4: Set $S = (t\Lambda)^{\frac{1}{2}} V$;
 - 5: Set $H = \text{diag}\left\{\frac{1}{1+t\Lambda_{1,1}}, \dots, \frac{1}{1+t\Lambda_{m,m}}\right\}$;
 - 6: Return (S, H) .
-

Remark. The time complexity of this sketched updating strategy is $O(m^2 d)$ per round because of the orthonormalizing operation. One can update the sketch every m rounds to improve time complexity to $O(md)$ [30].

Last, we discuss the asymmetric query strategy in SOA3. In Section 2.4, we compute variance $v_t = x_t^\top \Sigma_t x_t$ to enhance the query strategy. For the same purpose, in SOA3, we compute variance based on Eq. (13):

$$v_t = x_t^\top (I_d - S_{t-1}^\top H_{t-1} S_{t-1}) x_t. \quad (18)$$

Based on Eq. (18) and Algo. 3, we summarize the sketched query strategy in Algo. 6.

4.2 Sparse Sketched Algorithm

In many real-world applications, data is sparse that $\|x_t\|_0 \leq s$ for all t , and $s \ll d$ is a small constant. For most first-order online methods, computational complexities depend on s rather than d . However, SOA3 cannot enjoy this sparsity, because the sketch matrix S_t will become dense quickly due to the orthonormalizing updating of V_t . To address this, we propose a sparse variant of SOA3 to achieve a purely sparsity-dependent time cost, named Sparse Sketched Online Adaptive Asymmetric (SSOA3) Learning.

The key of SSOA3 is to decompose the estimated eigenvectors V_t and predictive vector μ_t so that they can keep sparse. Specifically, there are two main modifications: (1) the eigenvectors V_t are modified as $V_t = F_t U_t$, where $F_t \in \mathbb{R}^{m \times m}$ is an orthonormalizing matrix so that $F_t U_t$ is orthonormal, and $U_t \in \mathbb{R}^{m \times d}$ is a sparsely updatable

1. For sake of simplicity, $V_t + \Gamma_{t+1} V_t \hat{x}_t \hat{x}_t^\top$ is assumed as full rank with rows all the way, so that the " $\xleftarrow{\text{orth}}$ " operation always keeps the same dimensionality of V_t .

Algorithm 6 Sketched Asymmetric Query Strategy: **Sketch-Query**(p_t).

Input $\rho_{max} = \max\{1, \rho\}$; query bias (δ_+, δ_-) for positive and negative predictions.

- 1: Compute the variance $v_t = x_t^\top (I_d - S_{t-1}^\top H_{t-1} S_{t-1}) x_t$;
- 2: Compute the query parameter $q_t = |p_t| - \frac{1}{2} \frac{\eta \rho_{max}}{v_t + \gamma}$;
- 3: **if** $q_t \leq 0$ **then**
- 4: Set $q_t = 0$;
- 5: **end if**
- 6: **if** $p_t \geq 0$ **then**
- 7: $p_t^+ = \frac{\delta_+}{\delta_+ + q_t}$;
- 8: Draw a Bernoulli variable $Z_t \in \{0, 1\}$ with p_t^+ .
- 9: **else**
- 10: $p_t^- = \frac{\delta_-}{\delta_- + q_t}$;
- 11: Draw a Bernoulli variable $Z_t \in \{0, 1\}$ with p_t^- .
- 12: **end if**
- 13: **Return** Z_t .

direction. (2) the weight μ_t are split as $\bar{\mu}_t + U_{t-1}^\top b_t$, where $b_t \in \mathbb{R}^m$ maintains the weight on the subspace captured by V_{t-1} (the same as U_{t-1}), and $\bar{\mu}_t$ captures the weight on the complementary subspace.

Next, we describe the way to update $\bar{\mu}_t$ and b_t sparsely in detail. Firstly, according to Eq. (14) and $S_t = (t\Lambda)^{\frac{1}{2}} V_t = (t\Lambda)^{\frac{1}{2}} F_t U_t$, we have:

$$\begin{aligned} \mu_{t+1} &= \mu_t - \eta(I_d - S_t^\top H_t S_t) g_t \\ &= \bar{\mu}_t + U_{t-1}^\top b_t - \eta g_t + \eta U_t^\top F_t^\top (t\Lambda H_t) F_t U_t g_t \\ &= [\underbrace{\bar{\mu}_t - \eta g_t - (U_t - U_{t-1})^\top b_t}_{\bar{\mu}_{t+1}}] + U_t^\top [\underbrace{b_t + \eta F_t^\top (t\Lambda H_t) F_t U_t g_t}_{b_{t+1}}]. \end{aligned}$$

Based on this equation, we define the updating rule of $\bar{\mu}_t$:

$$\bar{\mu}_{t+1} = \bar{\mu}_t - \eta g_t - (U_t - U_{t-1})^\top b_t,$$

and define the updating rule of b_t :

$$b_{t+1} = b_t + \eta F_t^\top (t\Lambda H_t) F_t U_t g_t.$$

Based on the above, we summarize SSOA3 in Algo. 7, where the pseudo-code of sparse Oja's algorithms is provided in Supplementary B.2 due to the page limitation.

Next, we discuss how to update Λ_t , U_t and F_t . First, we rewrite Eq. (15) based on $V_t = F_t U_t$:

$$\Lambda_t = (I_m - \Gamma_t) \Lambda_{t-1} + \Gamma_t \text{diag}\{F_{t-1} U_{t-1} \hat{x}_t\}^2.$$

and rewrite Eq. (16) in the same way:

$$\begin{aligned} F_t U_t &\stackrel{\text{orth}}{\leftarrow} F_{t-1} U_{t-1} + \Gamma_t F_{t-1} U_{t-1} \hat{x}_t \hat{x}_t^\top, \\ &= F_{t-1} (U_{t-1} + F_{t-1}^{-1} \Gamma_t F_{t-1} U_{t-1} \hat{x}_t \hat{x}_t^\top), \end{aligned}$$

where $U_t = U_{t-1} + \delta_t \hat{x}_t^\top$ and $\delta_t = F_{t-1}^{-1} \Gamma_t F_{t-1} U_{t-1} \hat{x}_t$. Note that $U_t - U_{t-1}$ is a sparse rank-one matrix, which makes the update of $\bar{\mu}_t$ efficient.

Since the update of F_t is to enforce $F_t U_t$ orthonormal, we apply the Gram-Schmidt algorithm to F_{t-1} in a Banach space, where the inner product is defined as $\langle a, b \rangle = a^\top K_t b$ and $K_t = U_t U_t^\top$ is the Gram matrix (see Supplementary

Algorithm 7 Sparse Sketched Online Adaptive Asymmetric Active (SSOA3) Learning Algorithm.

Input budget B ; learning rate η ; regularized parameter γ ; sketch size m ; bias $\rho = \frac{\alpha_p * T_n}{\alpha_n * T_p}$ for "sum", $\rho = \frac{c_p}{c_n}$ for "cost".

Initialization $\bar{\mu}_1 = 0_{d \times 1}$, $b_1 = 0_{m \times 1}$, $B_1 = 0$;

Initialization $(\Lambda_0, F_0, U_0, H_0) \leftarrow \text{SparseSketchInit}(m)$;

- 1: **for** $t = 1 \rightarrow T$ **do**
- 2: Receive sample x_t ;
- 3: Compute $p_t = \mu_t^\top x_t$;
- 4: Make the prediction $\hat{y}_t = \text{sign}(p_t)$;
- 5: Draw a variable $Z_t = \text{SparseSketchQuery}(p_t) \in \{0, 1\}$;
- 6: **if** $Z_t = 1$ and $B_t < B$ **then**
- 7: Query the true label $y_t \in \{-1, +1\}$, $B_{t+1} = B_t + 1$;
- 8: Compute the loss $\ell_t(\mu_t)$, based on Equation (4);
- 9: Compute the t -sketch vector $\hat{x}_t = \frac{x_t}{\sqrt{\gamma}}$;
- 10: $(\Lambda_t, F_t, U_t, H_t, \delta_t) \leftarrow \text{SparseSketchUpdate}(\hat{x}_t)$;
- 11: **if** $\ell_t(\mu_t) > 0$ **then**
- 12: $\bar{\mu}_{t+1} = \bar{\mu}_t - \eta g_t - \hat{x}_t \delta_t^\top b_t$, where $g_t = \partial \ell_t(\mu_t)$;
- 13: $b_{t+1} = b_t + \eta F_t^\top (t\Lambda_t H_t) F_t U_t g_t$;
- 14: $\mu_{t+1} = \bar{\mu}_{t+1} + U_t^\top b_{t+1}$;
- 15: **else**
- 16: $\mu_{t+1} = \mu_t$, $\bar{\mu}_{t+1} = \bar{\mu}_t$, $b_{t+1} = b_t$;
- 17: **end if**
- 18: **else**
- 19: $\mu_{t+1} = \mu_t$, $\bar{\mu}_{t+1} = \bar{\mu}_t$, $b_{t+1} = b_t$, $B_{t+1} = B_t$;
- 20: $(\Lambda_t, F_t, U_t, H_t, \delta_t) = (\Lambda_{t-1}, F_{t-1}, U_{t-1}, H_{t-1}, \delta_{t-1})$.
- 21: **end if**
- 22: **end for**

B.2). Consequently, we can update K_t efficiently based on the update of U_t :

$$\begin{aligned} K_t &= U_t U_t^\top, \\ &= (U_{t-1} + \delta_t \hat{x}_t^\top) (U_{t-1} + \delta_t \hat{x}_t^\top)^\top, \\ &= K_{t-1} + U_{t-1} \hat{x}_t \delta_t^\top + \delta_t \hat{x}_t^\top U_{t-1}^\top + \delta_t \hat{x}_t^\top \hat{x}_t \delta_t^\top. \end{aligned}$$

We summarize the Sparse Oja's algorithm for OA3 in Supplementary B.2.

Remark. Note that both the updates of $\bar{\mu}_t$ and b_t require $O(m^2 + ms)$ time complexity. The most time-consuming step is the update of F_t , which needs $O(m^3)$. Furthermore, the prediction $\mu_t^\top x_t = \bar{\mu}_t^\top x_t + b_t^\top U_{t-1} x_t$ can be computed in $O(ms)$ time. So, the overall time complexity of the sparse sketched update rule is $O(m^3 + ms)$.

Like SOA3, SSOA3 also computes the variance v_t in an approximate way. Based on the decomposition of estimated eigenvectors $V_t = F_t U_t$ and Eq. (18), we have:

$$v_t = x_t^\top (I_d - U_{t-1}^\top F_{t-1}^\top (t-1) \Lambda_{t-1} H_{t-1} F_{t-1} U_{t-1}) x_t.$$

Based on this equation and Algo. 3, we summarize the sparse sketched asymmetric query strategy in Supplementary B.2.

5 EXPERIMENTS

In this section, we evaluate the performance and characteristics of the proposed algorithms².

2. The codes will be released in <https://github.com/Vanint/OA3>.

5.1 Experimental Testbed and Setup

We compare **OA3** and its variants (**OA3_{diag}**, **SOA3**, **SSOA3**) with several state-of-the-art online active learning methods: (1) Online Passive-aggressive Active Algorithm (**PAA**) [31]; (2) Online Asymmetric Active Algorithm (**OAAL**) [4]; (3) Cost-Sensitive Online Active Algorithm (**CSOAL**) [5]; (4) Second-order Online Active Algorithm (**SOAL**) [32] and its cost-sensitive variant (**SOAL-CS**) [32].

All algorithms are evaluated on four benchmark datasets. The statistics are summarized in Table 1. Specifically, the first three datasets are obtained from LIBSVM³ and the fourth dataset is obtained from KDD Cup 2008⁴.

For data preprocessing, all samples are normalized by $x_t \leftarrow \frac{x_t}{\|x_t\|_2}$, which is extensively used in online learning, since samples are obtained sequentially. When budgets are run out, both the query and update of the corresponding method will stop.

For fair comparisons, all algorithms use the same experimental settings. We set $\alpha_p = \alpha_n = 0.5$ for *sum*, and $c_p = 0.9$ and $c_n = 0.1$ for *cost*. The value of ρ is set to $\frac{\alpha_p * T_n}{\alpha_n * T_p}$ for *sum* and $\frac{c_p}{c_n}$ for *cost*. In addition, query biases ($\delta, \delta_+, \delta_-$) and learning rates η for all algorithms are selected from $[10^{-5}, 10^{-4}, \dots, 10^4, 10^5]$ using cross validations. By default, the regularization parameter γ is set to 1 for all second order algorithms (*i.e.*, **SOAL** and **OA3** based algorithms). For our sketched algorithms, we focus on the case that the sketch size m is fixed as 5, although our methods can be easily generalized by setting different sketch size like [20], while other implementation details are similar to [20].

On each dataset, experiments are conducted over 20 random permutations of data. Results are averaged over these 20 runs and 4 metrics are employed: *sensitivity*, *specificity*, weighted *sum* of sensitivity and specificity, and weighted *cost* of misclassification. All algorithms are implemented in MATLAB on a 3.40GHz Windows machine.

TABLE 1: Datasets for Evaluation of OA3 Algorithms

Dataset	#Examples	#Features	#Pos:#Neg
protein	17766	357	1:1.7
Sensorless	58509	48	1:10
w8a	64700	300	1:32.5
KDDCUP08	102294	117	1:163.19

5.2 Evaluation on Fixed Query Budgets

We first evaluate all algorithms under fixed budgets. Figs. 1 and 2 show the development of *sum* and *cost* performance, respectively and Table 2 summarizes more details.

First, **OAAL** (asymmetric query) and **CSOAL** (asymmetric update) outperform **PAA** (symmetric rule) in most cases. This comparison shows the importance of asymmetric strategies for imbalanced data in online active learning.

Second, as expected, all second order based algorithms (**SOAL** and **OA3**) outperform the first-order algorithms (**PAA**, **OAAL** and **CSOAL**) in most cases, which confirms the effectiveness of second-order information.

Third, the proposed **OA3** algorithms outperform all baselines with smaller standard deviations, which demonstrates the effectiveness and stability of our methods.

3. <https://www.csie.ntu.edu.tw/~cjlin/libsvmtools/datasets/>.
4. <http://www.kdd.org/kdd-cup/view/kdd-cup-2008/Data>.

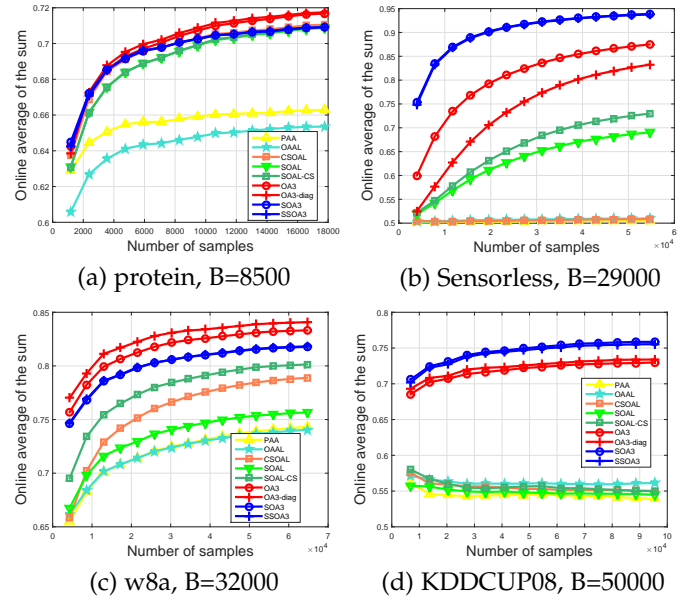


Fig. 1: Evaluation of sum with fixed budget.

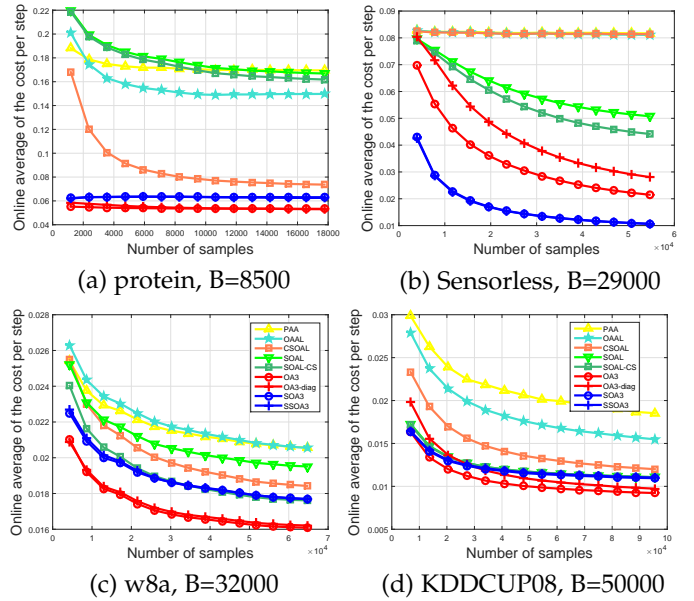


Fig. 2: Evaluation of cost with fixed budget.

According to comparisons in terms of *sensitivity* and *specificity*, our proposed algorithms achieve the best *sensitivity* on all datasets and produce fairly good *specificity* on most datasets. This indicates that our algorithms pay more attention to minority samples, which are usually more important in practical tasks.

Last, we compare the efficiency of the proposed methods. From Table 2, **OA3_{diag}**, **SOA3** and **SSOA3** are much efficient than the original **OA3** with quite slight performance degradation. Specifically, when datasets are quite high-dimensional, **SOA3** and **SSOA3** are further faster than **OA3_{diag}**. These observations imply that **SOA3** and **SSOA3** are better choices for balancing performance and efficiency.

5.3 Evaluation on Varying Query Budgets

In this subsection, we compare the performance of all algorithms with varying query budgets. Figs. 3 and 4 show the results in terms of *sum* and *cost* respectively.

TABLE 2: Evaluation of the OA3 algorithms

Algorithm	"sum" on protein				"cost" on protein			
	Sum(%)	Sensitivity(%)	Specificity (%)	Time(s)	Cost	Sensitivity(%)	Specificity (%)	Time(s)
PAA	66.263 ± 0.553	61.455 ± 4.455	71.072 ± 3.732	0.274	3092.285 ± 248.215	61.882 ± 3.777	70.754 ± 3.357	0.274
OAAL	65.930 ± 0.574	68.953 ± 3.442	62.907 ± 3.664	0.275	2657.710 ± 210.120	67.306 ± 3.142	74.343 ± 2.305	0.277
CSOAL	71.073 ± 0.304	69.565 ± 3.144	72.582 ± 2.714	0.258	1309.025 ± 75.994	89.110 ± 1.285	47.167 ± 2.204	0.263
SOAL	70.863 ± 0.734	62.576 ± 5.437	79.150 ± 4.177	12.411	2959.845 ± 356.434	62.586 ± 5.356	79.163 ± 4.104	13.095
SOAL-CS	70.920 ± 0.734	63.115 ± 5.490	78.725 ± 4.268	12.616	2876.015 ± 370.944	63.853 ± 5.600	78.152 ± 4.478	13.736
OA3	71.673 ± 0.348	72.608 ± 4.700	70.738 ± 4.838	12.511	949.855 ± 5.615	99.691 ± 0.099	3.106 ± 0.963	8.870
OA3 _{diag}	71.531 ± 0.334	72.114 ± 1.270	70.949 ± 1.393	7.008	938.795 ± 9.116	99.144 ± 0.188	8.480 ± 1.864	5.318
SOA3	71.028 ± 0.247	70.658 ± 2.766	71.398 ± 2.485	1.395	1117.690 ± 38.451	95.041 ± 0.912	21.421 ± 3.461	1.360
SSOA3	70.907 ± 0.304	70.197 ± 3.102	71.616 ± 2.967	1.004	1137.265 ± 45.136	94.474 ± 0.971	23.749 ± 3.238	0.944

Algorithm	"sum" on Sensorless				"cost" on Sensorless			
	Sum(%)	Sensitivity(%)	Specificity (%)	Time(s)	Cost	Sensitivity(%)	Specificity (%)	Time(s)
PAA	50.411 ± 0.487	8.049 ± 9.730	92.772 ± 8.926	0.426	4789.080 ± 85.260	11.395 ± 14.573	89.707 ± 14.189	0.432
OAAL	51.661 ± 0.377	39.208 ± 0.790	64.114 ± 0.683	0.441	4809.425 ± 40.441	38.309 ± 0.874	65.102 ± 0.578	0.445
CSOAL	50.582 ± 0.279	9.172 ± 8.983	91.993 ± 8.670	0.405	4774.760 ± 30.883	7.069 ± 2.585	93.870 ± 1.949	0.409
SOAL	69.381 ± 1.524	40.079 ± 3.141	98.683 ± 0.179	0.826	2904.685 ± 145.436	40.854 ± 3.215	98.621 ± 0.298	0.824
SOAL-CS	73.426 ± 1.118	49.253 ± 2.339	97.598 ± 0.338	0.874	2555.670 ± 113.284	49.267 ± 2.570	97.612 ± 0.362	0.871
OA3	87.944 ± 0.516	89.649 ± 0.973	86.238 ± 1.148	0.966	1219.940 ± 57.251	89.113 ± 0.948	86.863 ± 0.844	0.985
OA3 _{diag}	86.268 ± 0.744	87.469 ± 2.042	85.067 ± 1.374	0.792	1364.925 ± 63.246	87.365 ± 1.190	85.710 ± 1.682	0.761
SOA3	94.067 ± 0.238	95.860 ± 0.318	92.274 ± 0.578	0.862	607.540 ± 34.277	95.458 ± 0.484	92.666 ± 0.823	0.863
SSOA3	94.011 ± 0.349	95.870 ± 0.394	92.151 ± 0.747	0.920	605.860 ± 29.903	95.441 ± 0.472	92.713 ± 0.707	0.913

Algorithm	"sum" on w8a				"cost" on w8a			
	Sum(%)	Sensitivity(%)	Specificity (%)	Time(s)	Cost	Sensitivity(%)	Specificity (%)	Time(s)
PAA	74.121 ± 1.196	57.716 ± 2.564	90.526 ± 0.213	0.990	1334.555 ± 29.329	57.512 ± 2.309	90.514 ± 0.270	0.982
OAAL	73.919 ± 0.848	57.850 ± 1.798	89.987 ± 0.163	1.022	1327.965 ± 16.675	56.945 ± 1.033	90.776 ± 0.040	1.034
CSOAL	78.929 ± 0.586	68.078 ± 1.307	89.780 ± 0.159	0.976	1193.555 ± 11.979	66.699 ± 0.967	90.214 ± 0.110	0.979
SOAL	75.688 ± 0.531	60.476 ± 1.071	90.899 ± 0.042	3.340	1262.290 ± 17.663	60.212 ± 1.031	90.917 ± 0.028	3.458
SOAL-CS	80.076 ± 0.380	69.912 ± 0.781	90.241 ± 0.050	3.763	1137.000 ± 14.635	69.268 ± 0.944	90.403 ± 0.053	3.752
OA3	83.313 ± 0.951	84.369 ± 0.565	82.257 ± 2.365	14.118	1042.260 ± 7.455	79.240 ± 0.679	89.149 ± 0.194	9.002
OA3 _{diag}	84.129 ± 0.260	83.101 ± 0.435	85.157 ± 0.742	6.691	1048.075 ± 7.826	79.020 ± 0.477	89.117 ± 0.126	5.398
SOA3	81.759 ± 0.455	80.864 ± 0.760	82.655 ± 1.303	4.556	1150.620 ± 10.609	76.234 ± 0.974	88.256 ± 0.266	4.364
SSOA3	81.803 ± 0.265	80.365 ± 0.788	83.241 ± 0.816	3.398	1149.620 ± 8.379	76.079 ± 0.946	88.315 ± 0.273	3.332

Algorithm	"sum" on KDDCUP08				"cost" on KDDCUP08			
	Sum(%)	Sensitivity(%)	Specificity (%)	Time(s)	Cost	Sensitivity(%)	Specificity (%)	Time(s)
PAA	53.433 ± 4.439	48.475 ± 8.820	58.391 ± 2.286	1.065	1863.705 ± 155.865	23.900 ± 2.803	85.866 ± 1.624	1.082
OAAL	56.054 ± 1.589	27.006 ± 2.978	85.101 ± 1.273	1.034	1567.705 ± 72.265	21.701 ± 3.897	88.899 ± 0.845	1.045
CSOAL	55.891 ± 3.842	25.257 ± 8.550	86.526 ± 1.625	0.938	1206.975 ± 27.689	13.756 ± 1.855	92.885 ± 0.275	0.974
SOAL	53.768 ± 2.346	26.942 ± 5.182	80.594 ± 1.574	3.292	1126.580 ± 37.343	9.222 ± 0.525	93.926 ± 0.390	5.879
SOAL-CS	54.775 ± 2.515	28.363 ± 5.433	81.188 ± 1.693	3.468	1129.770 ± 36.692	9.342 ± 0.543	93.888 ± 0.383	5.935
OA3	73.189 ± 2.510	90.859 ± 2.354	55.520 ± 3.729	7.066	931.645 ± 60.664	35.947 ± 1.946	94.369 ± 0.507	4.467
OA3 _{diag}	73.598 ± 2.144	87.844 ± 1.286	59.353 ± 3.817	2.699	977.920 ± 13.775	38.644 ± 1.276	93.765 ± 0.119	2.708
SOA3	74.200 ± 1.088	88.965 ± 1.810	59.434 ± 3.124	3.779	1063.260 ± 13.663	25.939 ± 3.965	93.627 ± 0.285	3.928
SSOA3	75.642 ± 1.560	90.971 ± 1.329	60.313 ± 3.234	3.376	1056.040 ± 16.917	25.778 ± 2.852	93.706 ± 0.296	3.970

In detail, our algorithms achieve good performance over a wide range of budgets in terms of both metrics. This observation further demonstrates the effectiveness and stability of our algorithms. Moreover, it suggests that our algorithms can help real-world companies with different labeling budgets.

In addition, when the query budget falls, the standard deviation of each algorithm increases. This observation implies that the randomness of samples plays an important role in performance, especially when the budget is limited, which validates the importance of query strategies.

5.4 Evaluation of Algorithm Properties

We have evaluated performance of the proposed algorithms in previous experiments, where promising results confirm their superiority. Next, we further examine their unique properties, including the influence of query biases, cost weights and learning rates. The examinations contribute to better understanding and applications of the proposed methods. Due to the page limitation, we only report the

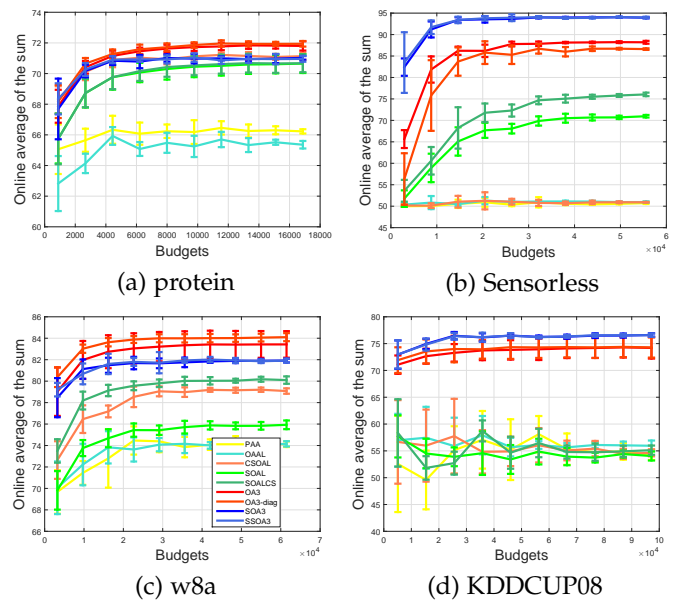


Fig. 3: Evaluation of sum with varying budgets.

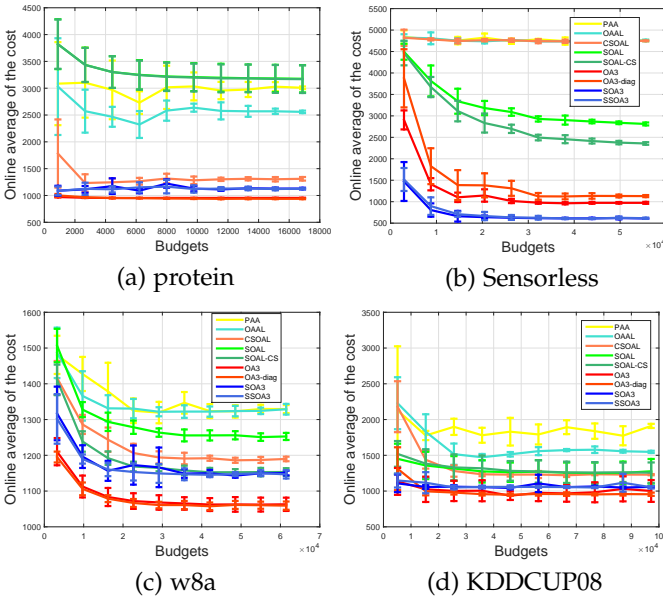


Fig. 4: Evaluation of cost with varying budgets.

results of *sum* metric, while more results based on *cost* metric are put in Supplementary C. Each experiment focuses on only one variable, while all other variable settings are fixed and similar with previous experiments.

5.4.1 Evaluation Between Query Biases

We first examine the influences of query biases on OA3 under a limited budget. All query biases (δ_+ , δ_-) are selected from $[10^{-5}, 10^{-4}, \dots, 10^4, 10^5]$.

The best results (i.e., deep red color in Fig. 5) are often obtained when $\delta_+ \in \{10^2, 10^3, 10^4, 10^5\}$ and $\delta_- \in \{1, 10\}$. This suggests, when querying more samples with the positive prediction (i.e., $\delta_+ \geq \delta_-$), OA3 can achieve better results. In other words, when paying more attention to positive predictions, the model will query more positive samples which are more informative in imbalanced tasks.

This observation is different from the discussions in OAAL [4], where the authors argued that δ_- should be larger than δ_+ . The main difference is that our algorithm considers asymmetric strategies in both optimization and queries; while OAAL considers only the asymmetric query. As a result, our method can query more positive samples (i.e., minority) due to the algorithm characteristics.

In addition, when both δ_+ and δ_- are large (i.e., the upper right corners in Fig. 5), our algorithms achieve fairly good performance. In this setting, the algorithm tends to query each observed sample and degrades to the ‘‘First come first served’’ strategy. This means that our algorithms with weak query strategy can also perform well. Moreover, when both δ_+ and δ_- are small (i.e., the bottom left corner), the model tends to ignore the samples, so the algorithm performance decreases significantly.

5.4.2 Evaluation of Cost Weights

In this subsection, we evaluate the influence of different cost weights, i.e., α_n , where $\alpha_p = 1 - \alpha_n$. Fig. 6 summarizes the results of *sum* metric under a fixed budget. We find that our proposed algorithms consistently outperform all other algorithms with different weights. This observation shows

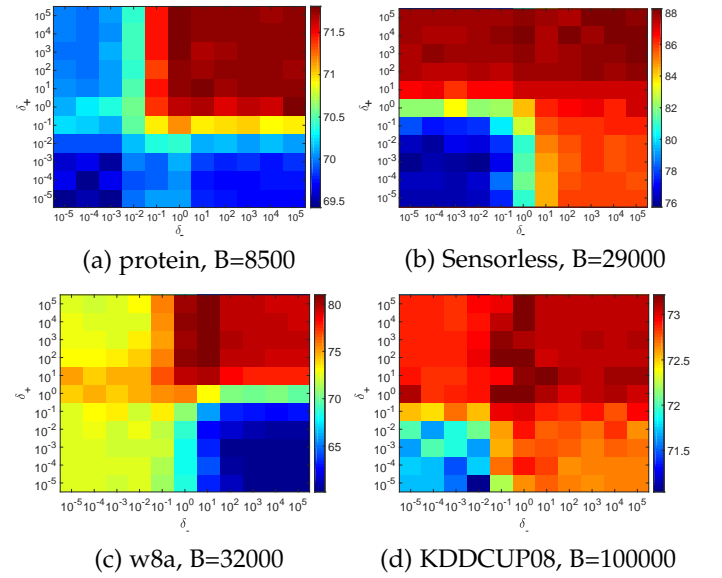


Fig. 5: Performance of sum with varying query parameters.

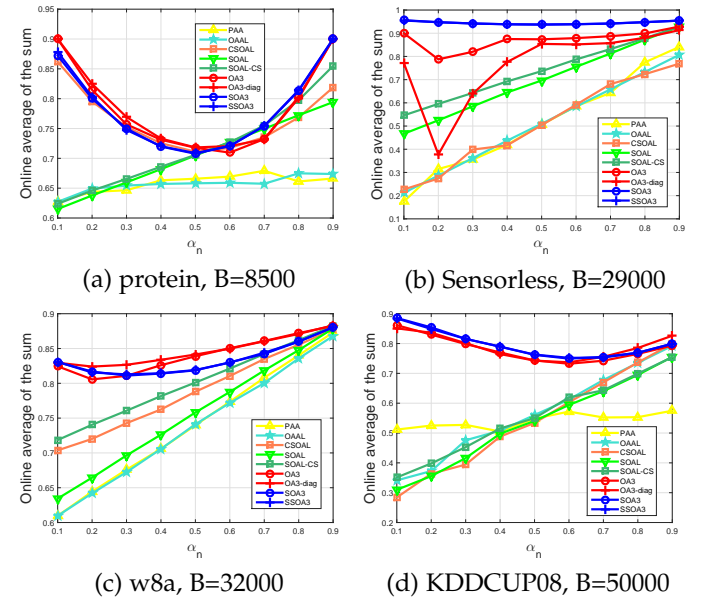


Fig. 6: Performance of sum with varying cost weights.

that OA3 based algorithms have a wide selection range of cost weights, which further validates the effectiveness of the proposed methods.

5.4.3 Evaluation of Learning Rates

We next evaluate the influence of different learning rates to the proposed methods, where the learning rate η is selected from $[10^{-4}, 10^{-3}, \dots, 10^3, 10^4]$.

Fig. 7 shows a suitable range of learning rates for different datasets, which provides a candidate choice of the learning rate for algorithm engineers. To be specific, OA3 algorithms achieve the best result on most datasets. Moreover, SOA3 and SSOA3 perform well on most datasets and sometimes even better than OA3. Considering that SOA3 and SSOA3 are more efficient than OA3, we conclude that the sketched versions of OA3 are favorable choices to balance performance and efficiency.

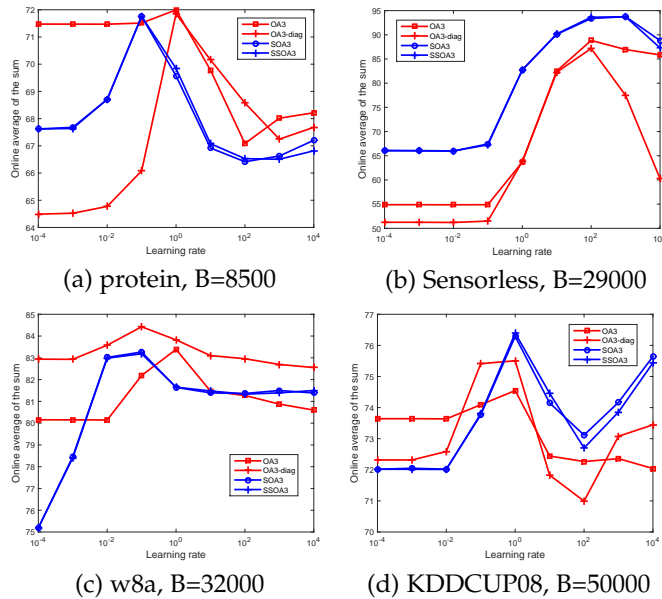


Fig. 7: Performance of sum with varying learning rates.

5.5 Evaluation on High Dimensional Datasets

In this subsection, we further evaluate our methods on two higher dimensional datasets (CIFAR-10⁵ and Internet Advertisements⁶ (IAD)). The dimensionality of CIFAR-10 is 3072 and that of IAD is 1558. To be specific, we construct the CIFAR-10 dataset by randomly sampling 20% samples from the CIFAR-10 training set, and randomly take one class as the positive class and set other classes as the negative class. All images ($\mathbb{R}^{32 \times 32 \times 3}$) are squeezed to the vectors (\mathbb{R}^{3072}). In addition, we clean IAD by removing the samples that have null attributes. Other settings are the same as the previous experiments. Due to the page limits, we only report the results of *sum* metric, while more results based on *cost* metric and additional analysis are put in Supplementary C.

As shown in Table 3, OA3-based algorithms achieve the best performance on both datasets. However, the running time of OA3 is much longer than first-order methods. In contrast, the proposed sketched variants (i.e., SOA3 and SSOA3) are much faster than OA3. Meanwhile, they also perform very well and sometimes even better than OA3. In this sense, SOA3 and SSOA3 are favorable choices when handling real-world high-dimensional datasets.

6 CONCLUSION

In this paper, we have proposed a novel online adaptive asymmetric active learning algorithm to handle imbalanced and unlabeled datastream under limited query budgets. Relying on samples' second-order information, we develop a new asymmetric strategy, which integrates both the asymmetric losses and query strategies. We theoretically analyze the mistake and cost-sensitive metric bounds of the proposed algorithm, for the cases within budgets and over budgets.

To overcome the time-consuming problem of second-order methods, we further propose a sketch variant of

our method, which can be developed as a sparse sketch approach. We empirically evaluate the proposed algorithms in real-world datasets. Promising results confirm the effectiveness, efficiency and stability of the proposed methods. In the future, we will extend the linear classifier to a nonlinear one with kernel methods.

7 ACKNOWLEDGEMENT

This work was partially supported by National Natural Science Foundation of China (NSFC) (61602185, 61502177 and 61876208), key project of NSFC (No. 61836003), Program for Guangdong Introducing Innovative and Entrepreneurial Teams 2017ZT07X183, Guangdong Provincial Scientific and Technological Funds (2018B010107001, 2017B090901008, 2017A010101011, 2017B090910005), Pearl River S&T Nova Program of Guangzhou 201806010081, Tencent AI Lab Rhino-Bird Focused Research Program (No. JR201902), CCF-Tencent Open Research Fund RAGR20170105, Program for Guangdong Introducing Innovative and Entrepreneurial Teams 2017ZT07X183.

REFERENCES

- [1] N. Abe, B. Zadrozny, J. Langford. Outlier detection by active learning. In *SIGKDD*, 2006, pp. 504-509.
- [2] S. C. Hoi, R. Jin, J. Zhu, M. R. Lyu. Batch mode active learning and its application to medical image classification. In *ICML*, 2006.
- [3] S. O. Moepya, S. S. Akhoury, F. V. Nelwamondo. Applying cost-sensitive classification for financial fraud detection under high class-imbalance. In *IEEE ICDM*, 2014, pp. 183-192.
- [4] X. Zhang, T. Yang, P. Srinivasan. Online asymmetric active learning with imbalanced data. In *SIGKDD*, 2016, pp. 2055-2064.
- [5] P. Zhao, S. C. Hoi. Cost-sensitive online active learning with application to malicious URL detection. In *SIGKDD*, 2013, pp. 919-927.
- [6] J. Wang, P. Zhao, S. C. Hoi. Exact soft confidence-weighted learning. In *ICML*, 2012, pp. 107-114.
- [7] M. Dunder, B. Krishnapuram, J. Bi, R. B. Rao. Learning classifiers when the training data is not IID. In *IJCAI*, 2007, pp. 756-761.
- [8] G. Hulten, L. Spencer, P. Domingos. Mining time-changing data streams. In *SIGKDD*, 2001, pp. 97-106.
- [9] N. Cesa-Bianchi, A. Conconi, C. Gentile. A second-order perceptron algorithm. *SIAM Journal on Computing*, 2005, No. 3, pp. 640-668.
- [10] J. Wang, P. Zhao and S. C. H. Hoi. Cost-sensitive online classification. *IEEE Transactions on Knowledge and Data Engineering*, 2014.
- [11] K. Crammer, O. Dekel, J. Keshet, S. Shalev-Shwartz, Y. Singer. Online passive-aggressive algorithms. *Journal of Machine Learning Research*, 2006, pp. 551-585.
- [12] Y. Freund, R. E. Schapire. Large margin classification using the perceptron algorithm. *Machine learning*, 1999, Vol. 37, pp. 277-296.
- [13] P. Zhao, S. C. Hoi. Cost-sensitive double updating online learning and its application to online anomaly detection. In *SIAM ICDM*, 2013, pp. 207-215.
- [14] N. Cesa-Bianchi, C. Gentile, L. Zaniboni. Worst-case analysis of selective sampling for linear classification. *Journal of Machine Learning Research*, 2006, No. 7, pp. 1205-1230.
- [15] V. S. Sheng, F. Provost, P. G. Ipeirotis. Get another label? improving data quality and data mining using multiple, noisy labels. In *SIGKDD*, 2008, pp. 614-622.
- [16] P. Zhao, Y. Zhang, M. Wu, S. C. Hoi, M. Tan, J. Huang. Adaptive cost-sensitive online classification. *IEEE Transactions on Knowledge and Data Engineering*, 2018.
- [17] K. Crammer, A. Kulesza, M. Dredze. Adaptive regularization of weight vectors. In *NeurIPS*, 2009, pp. 414-422.
- [18] K. Crammer, M. Dredze, F. Pereira. Exact convex confidence-weighted learning. In *NeurIPS*, 2009, pp. 345-352.
- [19] P. Zhao, F. Zhuang, M. Wu, X. Li, S. C. H. Hoi. Cost-sensitive online classification with adaptive regularization and its applications. In *IEEE ICDM*, 2015, pp. 649-658.
- [20] H. Luo, A. Agarwal, N. Cesa-Bianchi. Efficient second order online learning by sketching. In *NeurIPS*, 2016, pp. 902-910.

5. <https://www.cs.toronto.edu/~kriz/cifar.html>6. <https://archive.ics.uci.edu/ml/datasets.php>

TABLE 3: Sum evaluation on high-dimensional datasets

Algorithm	"sum" on CIFAR-10				"sum" on IAD			
	Sum(%)	Sensitivity(%)	Specificity (%)	Time(s)	Sum(%)	Sensitivity(%)	Specificity (%)	Time(s)
PAA	54.271 ± 2.255	18.060 ± 15.303	90.482 ± 15.269	0.513	52.570 ± 3.171	14.216 ± 12.900	90.924 ± 6.777	0.064
OAAAL	63.510 ± 0.525	60.149 ± 1.977	66.872 ± 1.363	0.475	58.965 ± 1.420	55.123 ± 1.865	62.807 ± 2.379	0.061
CSOAL	56.331 ± 3.485	21.552 ± 14.413	91.110 ± 8.913	0.466	55.783 ± 5.938	19.338 ± 13.048	92.228 ± 1.235	0.059
SOAL	56.161 ± 0.765	18.229 ± 2.197	94.092 ± 0.863	529.586	74.496 ± 5.005	52.892 ± 10.550	96.099 ± 0.984	21.655
SOAL-CS	60.133 ± 0.839	27.582 ± 1.993	92.685 ± 0.532	584.077	78.259 ± 0.830	63.235 ± 2.127	93.282 ± 1.162	28.633
OA3	72.858 ± 0.561	79.393 ± 3.627	66.322 ± 3.994	1948.292	80.398 ± 0.624	76.201 ± 3.238	84.595 ± 2.594	44.674
OA3 _{diag}	64.992 ± 1.830	64.448 ± 8.104	65.535 ± 6.215	152.623	81.359 ± 0.514	79.926 ± 2.227	82.792 ± 2.307	10.355
SOA3	67.959 ± 2.945	69.463 ± 8.768	66.456 ± 10.743	66.739	81.484 ± 2.133	85.515 ± 6.608	77.453 ± 7.641	4.084
SSOA3	68.678 ± 2.049	70.308 ± 6.538	67.047 ± 8.636	52.126	82.101 ± 7.677	91.005 ± 5.876	73.197 ± 19.614	3.215

- [21] Woodruff, P. David. Sketching as a tool for numerical linear algebra. *Foundations and Trends in Theoretical Computer Science*, 2014.
- [22] G. Krummenacher, B. McWilliams, Y. Kilcher, J. M. Buhmann, N. Meinshausen. Scalable adaptive stochastic optimization using random projections. In *NeurIPS*, 2016, pp. 1750-1758.
- [23] D. Wang, P. Wu, P. Zhao, Y. Wu, C. Miao, S. C. Hoi. High-dimensional data stream classification via sparse online learning. In *IEEE ICDM*, 2014, pp. 1007-1012.
- [24] Y. Zhang, P. Zhao, J. Cao, W. Ma, J. Huang, Q. Wu, M. Tan. Online Adaptive Asymmetric Active Learning for Budgeted Imbalanced Data. In *SIGKDD*, 2018, pp. 2768-2777.
- [25] M. Zinkevich. Online convex programming and generalized infinitesimal gradient ascent. In *ICML*, 2003, pp. 928-936.
- [26] M. Dredze, K. Crammer, F. Pereira. Confidence-weighted linear classification. In *ICML*, 2008, 264-271.
- [27] R. Horn. Matrix analysis. *Cambridge University Express*, 1985.
- [28] E. Oja. Simplified neuron model as a principal component analyzer. *Journal of Mathematical biology*, 1982, pp. 267-273.
- [29] E. Oja, J. Karhunen. On stochastic approximation of the eigenvectors and eigenvalues of the expectation of a random matrix. *Journal of Mathematical Analysis and Applications*, 1985, vol. 106, pp. 69-84.
- [30] M. Hardt, E. Price, The noisy power method: A meta algorithm with application. In *NeurIPS*, 2014, pp. 2861-2869.
- [31] J. Lu, P. Zhao, S. C. Hoi. Online passive-aggressive active learning. *Machine Learning*, 2016, Vol. 103, No. 2, pp. 141-183.
- [32] S. Hao, J. Lu, P. Zhao, C. Zhang, S. C. Hoi, C. Miao. Second-order online active learning and its applications. *IEEE Transactions on Knowledge and Data Engineering*, 2017.
- [33] J. Attenberg, F. Provost. Why label when you can search? Alternatives to active learning for applying human resources to build classification models under extreme class imbalance. In *SIGKDD*, 2010, pp. 423-432.



Yifan Zhang is working toward the M.E. degree in the School of Software Engineering, South China University of Technology, China. He received the B.E. degree from the Southwest University, China, in 2017. His research interests are broadly in machine learning, with high self-motivation to design explainable and robust algorithms for data-limited problems and decision-making tasks.



Peilin Zhao is currently a Principal Researcher at Tencent AI Lab, China. Previously, he has worked at Rutgers University, Institute for Infocomm Research (I2R), Ant Financial Services Group. His research interests include: Online Learning, Deep Learning, Recommendation System, Automatic Machine Learning, etc. He has published over 90 papers in top venues, including JMLR, ICML, KDD, etc. He has been invited as a PC member, reviewer or editor for many international conferences and journals, such as ICML, JMLR, etc. He received his bachelor degree from Zhejiang University, and his Ph.D. degree from Nanyang Technological University.



Shuaicheng Niu is currently a Ph.D candidate in South China University of Technology (SCUT), China, School of Software Engineering. He received the Bachelor degree in mathematics from Southwest Jiaotong University (SWJTU), China, in 2018. His research interests include Machine Learning, Reinforcement Learning and Neural Network Architecture Search.



Qingyao Wu received the Ph.D. degree in computer science from the Harbin Institute of Technology, Harbin, China, in 2013. He was a Post-Doctoral Research Fellow with the School of Computer Engineering, Nanyang Technological University, Singapore, from 2014 to 2015. He is currently a Professor with the School of Software Engineering, South China University of Technology, Guangzhou, China. His current research interests include machine learning, data mining, big data research.



Jiezhong Cao is a master of the School of Software Engineering, South China University of Technology, China. He received the B.S. degree in statistics from the Guangdong University of Technology, China, 2017. His current research interests include machine learning, generative model.



Junzhou Huang is an Associate Professor in the Computer Science and Engineering department at the University of Texas at Arlington. He received the B.E. degree from Huazhong University of Science and Technology, China, the M.S. degree from Chinese Academy of Sciences, China, and the Ph.D. degree in Rutgers university. His major research interests include machine learning, computer vision and imaging informatics. He was selected as one of the 10 emerging leaders in multimedia and signal processing by the IBM T.J. Watson Research Center in 2010. He received the NSF CAREER Award in 2016.



Mingkui Tan received his Bachelor Degree in Environmental Science and Engineering in 2006 and Master degree in Control Science and Engineering in 2009, both from Hunan University in Changsha, China. He received the Ph.D. degree in Computer Science from Nanyang Technological University, Singapore, in 2014. From 2014-2016, he worked as a Senior Research Associate on computer vision in the School of Computer Science, University of Adelaide, Australia. Since 2016, he has been with the School of Software Engineering, South China University of Technology, China, where he is currently a Professor. His research interests include machine learning, sparse analysis, deep learning and large-scale optimization.

Online Adaptive Asymmetric Active Learning with Limited Budgets

Yifan Zhang, Peilin Zhao, Shuaicheng Niu, Qingyao Wu, Jiezhong Cao, Junzhou Huang, Mingkui Tan

Abstract—This supplemental file provides the proofs of theorems, some algorithms, additional experiments and the related work in our paper of "Online Adaptive Asymmetric Active Learning with Limited Budgets" [1].

Index Terms—Active Learning; Online Learning; Class Imbalance; Budgeted Query; Sketching Learning.

SECTION A PROOFS OF THEOREMS

This section presents the proofs for all the theorems. For convenience, we introduce the following notations:

$$M_t = \mathbb{I}_{(\hat{y}_t \neq y_t)}, \rho = \frac{\alpha_p T_n}{\alpha_n T_p} \text{ or } \frac{c_p}{c_n},$$

$$\rho_t = \rho \mathbb{I}_{(y_t = +1)} + \mathbb{I}_{(y_t = -1)}, \rho_{max} = \max\{1, \rho\}, \rho_{min} = \min\{1, \rho\}.$$

A.1 Proof of Lemma 1

Lemma 1. Let $(x_1, y_1), \dots, (x_T, y_T)$ be a sequence of input samples, where $x_t \in \mathbb{R}^d$ and $y_t \in \{-1, +1\}$ for all t . Let T_B be the round that runs out of the budgets, i.e., $B_{T_B+1} = B$. For any $\mu \in \mathbb{R}^d$ and any $\delta > 0$, OA3 algorithm satisfies:

$$\sum_{t=1}^{T_B} M_t Z_t (\delta + q_t) \leq \frac{\delta}{\rho_{min}} \sum_{t=1}^{T_B} \ell_t(\mu) + \frac{1}{\eta \rho_{min}} \text{Tr}(\Sigma_{T_B+1}^{-1}) \times [M(\mu) + (1 - \delta)^2 \|\mu\|^2],$$

where $M(\mu) = \max_t \|\mu_t - \mu\|^2$.

Proof A.1. Consider that OA3 queries a label but makes a mistake at the round t , so that $Z_t = 1$ and $M_t = 1$. Then, based on the adaptive asymmetric update strategy, we have:

$$\mu_{t+1} = \arg \min_{\mu} f_t(\mu, \Sigma) = \arg \min_{\mu} h_t(\mu),$$

where $h_t(\mu) = \frac{1}{2} \|\mu_t - \mu\|_{\Sigma_{t+1}^{-1}}^2 + \eta g_t^\top \mu$.

Since h_t is convex and continuous, one can easily obtain the following inequality:

$$\begin{aligned} \partial h_t(\mu_{t+1})^\top (\mu - \mu_{t+1}) \\ = [(\mu_{t+1} - \mu_t)^\top \Sigma_{t+1}^{-1} + \eta g_t^\top] (\mu - \mu_{t+1}) \geq 0, \forall \mu. \end{aligned}$$

Rearranging the inequality will give:

$$\begin{aligned} (\eta g_t)^\top (\mu_{t+1} - \mu) &\leq (\mu_{t+1} - \mu_t)^\top \Sigma_{t+1}^{-1} (\mu - \mu_{t+1}) \\ &= \frac{1}{2} \left[\|\mu_t - \mu\|_{\Sigma_{t+1}^{-1}}^2 - \|\mu_{t+1} - \mu\|_{\Sigma_{t+1}^{-1}}^2 \right. \\ &\quad \left. - \|\mu_t - \mu_{t+1}\|_{\Sigma_{t+1}^{-1}}^2 \right]. \end{aligned} \quad (1)$$

Now, we provide a lower bound for $g_t^\top (\mu_{t+1} - \mu)$. Since $\ell_t(\mu) = \rho_t \max(0, 1 - y_t x_t^\top \mu)$ is a convex function, and based on $g_t^\top = M_t (-\rho_t y_t x_t^\top)$ and

$$\partial h_t(\mu_{t+1}) = 0 \iff (\mu_{t+1} - \mu_t)^\top \Sigma_{t+1}^{-1} + \eta g_t^\top = 0, \quad (2)$$

we have:

$$\begin{aligned} g_t^\top (\mu_{t+1} - \mu) &= g_t^\top (\mu_{t+1} - \mu + \mu_t - \mu_t) \\ &= M_t (-\rho_t y_t x_t^\top \mu) + M_t (\rho_t y_t x_t^\top \mu) - \frac{1}{\eta} \|\mu_t - \mu_{t+1}\|_{\Sigma_{t+1}^{-1}}^2. \end{aligned} \quad (3)$$

Combining the above Equation (3) with the facts:

$$\rho_t M_t (-y_t x_t^\top \mu_t) = \rho_t M_t |y_t x_t^\top \mu_t| = \rho_t M_t |p_t|,$$

and

$$\delta \ell_t\left(\frac{\mu}{\delta}\right) \geq \delta \rho_t (1 - y_t x_t^\top \frac{\mu}{\delta}) \iff y_t x_t^\top \mu \geq \delta - \frac{\delta}{\rho_t} \ell_t\left(\frac{\mu}{\delta}\right),$$

we get the following bound for $g_t^\top (\mu_{t+1} - \mu_t)$, i.e.,

$$\begin{aligned} g_t^\top (\mu_{t+1} - \mu_t) \\ \geq \rho_t M_t |p_t| + \rho_t M_t \left[\delta - \frac{\delta}{\rho_t} \ell_t\left(\frac{\mu}{\delta}\right) \right] - \frac{1}{\eta} \|\mu_t - \mu_{t+1}\|_{\Sigma_{t+1}^{-1}}^2 \\ = \rho_t M_t (\delta + |p_t|) - M_t \delta \ell_t\left(\frac{\mu}{\delta}\right) - \frac{1}{\eta} \|\mu_t - \mu_{t+1}\|_{\Sigma_{t+1}^{-1}}^2. \end{aligned} \quad (4)$$

Combining Equations (1) and (4) will give the following important inequality:

$$\begin{aligned} M_t Z_t (\delta + |p_t|) &\leq \frac{Z_t}{2\eta \rho_t} \left[\|\mu_t - \delta \mu\|_{\Sigma_{t+1}^{-1}}^2 - \|\mu_{t+1} - \delta \mu\|_{\Sigma_{t+1}^{-1}}^2 \right. \\ &\quad \left. + \|\mu_t - \mu_{t+1}\|_{\Sigma_{t+1}^{-1}}^2 \right] + M_t Z_t \left[\frac{\delta}{\rho_t} \ell_t(\mu) \right], \end{aligned} \quad (5)$$

where we replace $\delta \mu$ with μ .

- Y. Zhang, S. Niu, J. Cao, Q. Wu and M. Tan are with South China University of Technology, China. E-mail: {sezyifan, senc, secaojiezhong}@mail.scut.edu.cn; {qyw, mingkuitan}@scut.edu.cn.
- P. Zhao and J. Huang are with Tencent AI Lab, China. Email: peilinzhao@hotmail.com; joelhuang@tencent.com.
- P. Zhao, S. Niu and Q. Wu are co-first authors; Corresponding to M. Tan.

Then, according to Equation (2), we have:

$$\begin{aligned}
\|\mu_t - \mu_{t+1}\|_{\Sigma_{t+1}^{-1}}^2 &= \eta^2 g_t^\top \Sigma_{t+1} g_t \\
&= M_t \eta^2 \rho_t^2 x_t^\top \Sigma_{t+1} x_t \\
&= M_t \eta^2 \rho_t^2 \left(x_t^\top \Sigma_t x_t - \frac{x_t^\top \Sigma_t x_t x_t^\top \Sigma_t x_t}{\gamma + x_t^\top \Sigma_t x_t} \right) \\
&= M_t \eta^2 \rho_t^2 \frac{\gamma v_t}{\gamma + v_t} \\
&= M_t \frac{\eta^2 \rho_t^2}{\frac{1}{\gamma} + \frac{1}{v_t}},
\end{aligned}$$

where we use the updating rule of Σ .

Then, according to $M_t \leq 1$ and $Z_t \leq 1$, we rearrange Equation (5):

$$\begin{aligned}
M_t Z_t (\delta + q_t) &= M_t Z_t (\delta + |p_t| + c_t) \\
&= M_t Z_t \left(\delta + |p_t| - \frac{1}{2} \frac{\eta \rho_{max}}{\frac{1}{\gamma} + \frac{1}{v_t}} \right) \\
&\leq M_t Z_t \left(\delta + |p_t| - \frac{1}{2} \frac{\eta \rho_t}{\frac{1}{\gamma} + \frac{1}{v_t}} \right) \\
&\leq \frac{Z_t}{2\eta\rho_t} \left[\|\mu_t - \delta\mu\|_{\Sigma_{t+1}^{-1}}^2 - \|\mu_{t+1} - \delta\mu\|_{\Sigma_{t+1}^{-1}}^2 \right] \\
&\quad + M_t Z_t \left[\frac{\delta}{\rho_t} \ell_t(\mu) \right] \\
&\leq \frac{Z_t}{2\eta\rho_t} \left[\|\mu_t - \delta\mu\|_{\Sigma_{t+1}^{-1}}^2 - \|\mu_{t+1} - \delta\mu\|_{\Sigma_{t+1}^{-1}}^2 \right] \\
&\quad + \frac{\delta}{\rho_{min}} \ell_t(\mu). \tag{6}
\end{aligned}$$

We highlight the analysis here provides the theoretical guarantees for the definition of query confidence c_t , which fascinates the theoretical studies of the proposed algorithm. Next, summing the first right term of above inequality over $t = 1, \dots, T_B$, we have:

$$\begin{aligned}
&\sum_{t=1}^{T_B} \frac{Z_t}{\rho_t} \left[\|\mu_t - \delta\mu\|_{\Sigma_{t+1}^{-1}}^2 - \|\mu_{t+1} - \delta\mu\|_{\Sigma_{t+1}^{-1}}^2 \right] \\
&\leq \frac{1}{\rho_{min}} \left\{ \|\mu_1 - \delta\mu\|_{\Sigma_2^{-1}}^2 + \sum_{t=2}^{T_B} \left[\|\mu_t - \delta\mu\|_{\Sigma_{t+1}^{-1}}^2 - \|\mu_t - \delta\mu\|_{\Sigma_t^{-1}}^2 \right] \right\} \\
&= \frac{1}{\rho_{min}} \left[\|\mu_1 - \delta\mu\|_{\Sigma_2^{-1}}^2 + \sum_{t=2}^{T_B} \|\mu_t - \delta\mu\|_{(\Sigma_{t+1}^{-1} - \Sigma_t^{-1})}^2 \right] \\
&\leq \frac{1}{\rho_{min}} \left[\|\mu_1 - \delta\mu\|^2 \lambda_{max}(\Sigma_2^{-1}) + \sum_{t=2}^{T_B} \|\mu_t - \delta\mu\|^2 \lambda_{max}(\Sigma_{t+1}^{-1} - \Sigma_t^{-1}) \right] \\
&\leq \frac{1}{\rho_{min}} \left[\|\mu_1 - \delta\mu\|^2 \text{Tr}(\Sigma_2^{-1}) + \sum_{t=2}^{T_B} \|\mu_t - \delta\mu\|^2 \text{Tr}(\Sigma_{t+1}^{-1} - \Sigma_t^{-1}) \right] \\
&\leq \frac{1}{\rho_{min}} \max_{t \leq T_B} \|\mu_t - \delta\mu\|^2 \text{Tr}(\Sigma_{T_B+1}^{-1}) \\
&\leq \frac{2}{\rho_{min}} [M(\mu) + (1 - \delta)^2 \|\mu\|^2] \text{Tr}(\Sigma_{T_B+1}^{-1}), \tag{7}
\end{aligned}$$

where $M(\mu) = \max_t \|\mu_t - \mu\|^2$ and $\lambda_{max}(\Sigma)$ is the largest eigenvalue of Σ .

Now, combining Inequalities (6) and (7), we can easily obtain:

$$\sum_{t=1}^{T_B} M_t Z_t (\delta + q_t) \leq \frac{\delta}{\rho_{min}} \sum_{t=1}^{T_B} \ell_t(\mu) + \frac{1}{\eta \rho_{min}} \text{Tr}(\Sigma_{T_B+1}^{-1}) \times [M(\mu) + (1 - \delta)^2 \|\mu\|^2].$$

Consider another situation that $M_t Z_t = 0$, and we can find above inequality still holds. As results, we conclude the proofs of Lemma 1.

A.2 Proof of Theorem 1

Theorem 1. Let $(x_1, y_1), \dots, (x_T, y_T)$ be a sequence of input samples, where $x_t \in \mathbb{R}^d$ and $y_t \in \{-1, +1\}$ for all t . Let T_B be the round that runs out of the budgets, i.e., $B_{T_B+1} = B$. For any $\mu \in \mathbb{R}^d$, the expected mistake number of OA3 within budgets is bounded by:

$$\begin{aligned}
\mathbb{E} \left[\sum_{t=1}^{T_B} M_t \right] &= \mathbb{E} \left[\sum_{\substack{t=1 \\ y_t=+1}}^{T_B} M_t + \sum_{\substack{t=1 \\ y_t=-1}}^{T_B} M_t \right] \\
&\leq \frac{1}{\rho_{min}} \left[\sum_{t=1}^{T_B} \ell_t(\mu) + \frac{1}{\eta} D(\mu) \text{Tr}(\Sigma_{T_B+1}^{-1}) \right],
\end{aligned}$$

where $D(\mu) = \max \left\{ \frac{M(\mu) + (1 - \delta_+)^2 \|\mu\|^2}{\delta_+}, \frac{M(\mu) + (1 - \delta_-)^2 \|\mu\|^2}{\delta_-} \right\}$.

Proof A.2. Considering that OA3 queries a label but makes a mistake at the round t , so that $Z_t = 1$ and $M_t = 1$, there are two scenarios. That is, $p_t \geq 0$ with $M_t Z_t = 1$ represents our estimated class of sample x_t is positive, but true label is negative; while $p_t < 0$ with $M_t Z_t = 1$ represents our estimated class of sample x_t is negative, but true label is positive.

First, if $p_t \geq 0$, based on Lemma 1, for any $\mu \in \mathbb{R}^d$ and any $\delta_+ > 0$, we have :

$$\sum_{\substack{t=1 \\ y_t=-1}}^{T_B} M_t Z_t (\delta_+ + q_t) \leq \frac{\delta_+}{\rho_{min}} \sum_{\substack{t=1 \\ y_t=-1}}^{T_B} \ell_t(\mu) + \frac{\mathbb{I}_{(y_t=-1)}}{\eta \rho_{min}} \times [M(\mu) + (1 - \delta_+)^2 \|\mu\|^2] \text{Tr}(\Sigma_{T_B+1}^{-1}).$$

One can easily prove that this inequality still holds for $M_t Z_t = 0$.

Now, we would like to remove the random variable Z_t . First, when the query parameter $q_t > 0$, taking the expectation over random variables $\mathbb{E}(Z_t) = \frac{\delta_+}{\delta_+ + q_t}$ for $p_t \geq 0$, we have:

$$\mathbb{E} \left[\sum_{\substack{t=1 \\ y_t=-1}}^{T_B} \delta_+ M_t \right] \leq \frac{\delta_+}{\rho_{min}} \sum_{\substack{t=1 \\ y_t=-1}}^{T_B} \ell_t(\mu) + \frac{\mathbb{I}_{(y_t=-1)}}{\eta \rho_{min}} \times [M(\mu) + (1 - \delta_+)^2 \|\mu\|^2] \text{Tr}(\Sigma_{T_B+1}^{-1}).$$

On the other hand, when the query parameter $q_t \leq 0$, we set $q_t = 0$, and the random variables satisfy $\mathbb{E}(Z_t) = 1$. Then, we find the above inequality still holds. In addition, one can easily prove this inequality holds for $M_t = 0$.

Now, we obtain:

$$\mathbb{E} \left[\sum_{\substack{t=1 \\ y_t=-1}}^{T_B} M_t \right] \leq \sum_{\substack{t=1 \\ y_t=-1}}^{T_B} \frac{\ell_t(\mu)}{\rho_{min}} + \frac{\mathbb{I}_{(y_t=-1)}}{\eta \rho_{min} \delta_+} \times [M(\mu) + (1 - \delta_+)^2 \|\mu\|^2] \text{Tr}(\Sigma_{T_B+1}^{-1}). \quad (8)$$

Similarly, when $p_t < 0$, for any $\mu \in \mathbb{R}^d$ and any $\delta_- > 0$, we obtain:

$$\mathbb{E} \left[\sum_{\substack{t=1 \\ y_t=+1}}^{T_B} M_t \right] \leq \sum_{\substack{t=1 \\ y_t=+1}}^{T_B} \frac{\ell_t(\mu)}{\rho_{min}} + \frac{\mathbb{I}_{(y_t=+1)}}{\eta \rho_{min} \delta_-} \times [M(\mu) + (1 - \delta_-)^2 \|\mu\|^2] \text{Tr}(\Sigma_{T_B+1}^{-1}). \quad (9)$$

Summing Equations (8) and (9) will give:

$$\begin{aligned} \mathbb{E} \left[\sum_{t=1}^{T_B} M_t \right] &= \mathbb{E} \left[\sum_{\substack{t=1 \\ y_t=+1}}^{T_B} M_t + \sum_{\substack{t=1 \\ y_t=-1}}^{T_B} M_t \right] \\ &\leq \sum_{t=1}^{T_B} \frac{\ell_t(\mu)}{\rho_{min}} + \frac{1}{\eta \rho_{min}} D(\mu) \text{Tr}(\Sigma_{T_B+1}^{-1}) \\ &= \frac{1}{\rho_{min}} \left[\sum_{t=1}^{T_B} \ell_t(\mu) + \frac{1}{\eta} D(\mu) \text{Tr}(\Sigma_{T_B+1}^{-1}) \right], \end{aligned}$$

where $D(\mu) = \max \left\{ \frac{M(\mu) + (1 - \delta_+)^2 \|\mu\|^2}{\delta_+}, \frac{M(\mu) + (1 - \delta_-)^2 \|\mu\|^2}{\delta_-} \right\}$. Then, we conclude the proofs of Theorem 1.

A.3 Proof of Theorem 2

Theorem 2. Under the same condition in Theorem 1, by setting $\rho = \frac{\alpha_p T_n}{\alpha_n T_p}$, the proposed OA3 within budgets satisfies for any $\mu \in \mathbb{R}^d$:

$$\mathbb{E} [sum] \geq 1 - \frac{\alpha_n \rho_{max}}{T_n \rho_{min}} \left[\sum_{t=1}^{T_B} \ell_t(\mu) + \frac{1}{\eta} D(\mu) \text{Tr}(\Sigma_{T_B+1}^{-1}) \right].$$

Proof A.3. According to Equation (9), we have:

$$\mathbb{E} \left[\sum_{\substack{t=1 \\ y_t=+1}}^{T_B} \rho M_t \right] \leq \sum_{\substack{t=1 \\ y_t=+1}}^{T_B} \frac{\rho \ell_t(\mu)}{\rho_{min}} + \frac{\rho \mathbb{I}_{(y_t=+1)}}{\eta \rho_{min} \delta_-} \times [M(\mu) + (1 - \delta_-)^2 \|\mu\|^2] \text{Tr}(\Sigma_{T_B+1}^{-1}).$$

Now, combining with Equation (8) will give:

$$\begin{aligned} \mathbb{E} \left[\sum_{t=1}^{T_B} \rho_t M_t \right] &= \mathbb{E} \left[\sum_{\substack{t=1 \\ y_t=+1}}^{T_B} \rho M_t + \sum_{\substack{t=1 \\ y_t=-1}}^{T_B} M_t \right] \\ &\leq \frac{\max\{1, \rho\}}{\rho_{min}} \left[\sum_{t=1}^{T_B} \ell_t(\mu) + \frac{1}{\eta} D(\mu) \text{Tr}(\Sigma_{T_B+1}^{-1}) \right] \\ &= \frac{\rho_{max}}{\rho_{min}} \left[\sum_{t=1}^{T_B} \ell_t(\mu) + \frac{1}{\eta} D(\mu) \text{Tr}(\Sigma_{T_B+1}^{-1}) \right]. \end{aligned} \quad (10)$$

Now, from the definition of the weighted *sum*, we have:

$$\begin{aligned} \mathbb{E} \left[\sum_{t=1}^{T_B} \rho_t M_t \right] &= \rho \mathbb{E} [M_p] + \mathbb{E} [M_n] = \left(\frac{\alpha_p T_n}{\alpha_n T_p} \right) \mathbb{E} [M_p] + \mathbb{E} [M_n] \\ &= \frac{T_n}{\alpha_n} \left[\alpha_p \frac{\mathbb{E} [M_p]}{T_p} + \alpha_n \frac{\mathbb{E} [M_n]}{T_n} \right] = \frac{T_n}{\alpha_n} \left(1 - \mathbb{E} [sum] \right), \end{aligned} \quad (11)$$

where we used $\alpha_p + \alpha_n = 1$.

Combining Equations (10) and (11), we have:

$$\mathbb{E} [sum] \geq 1 - \frac{\alpha_n \rho_{max}}{T_n \rho_{min}} \left[\sum_{t=1}^{T_B} \ell_t(\mu) + \frac{1}{\eta} D(\mu) \text{Tr}(\Sigma_{T_B+1}^{-1}) \right].$$

Then, we conclude Theorem 2.

A.4 Proof of Theorem 3

Theorem 3. Under the same condition in Theorem 1, by setting $\rho = \frac{c_p}{c_n}$, the proposed OA3 within budgets satisfies for any $\mu \in \mathbb{R}^d$:

$$\mathbb{E} [cost] \leq \frac{c_n \rho_{max}}{\rho_{min}} \left[\sum_{t=1}^{T_B} \ell_t(\mu) + \frac{1}{\eta} D(\mu) \text{Tr}(\Sigma_{T_B+1}^{-1}) \right].$$

Proof A.4. From the definition of *cost* metric, we have:

$$\begin{aligned} \mathbb{E} \left[\sum_{t=1}^{T_B} \rho_t M_t \right] &= \rho \mathbb{E} [M_p] + \mathbb{E} [M_n] = \frac{c_p}{c_n} \mathbb{E} [M_p] + \mathbb{E} [M_n] \\ &= \frac{1}{c_n} (c_p \mathbb{E} [M_p] + c_n \mathbb{E} [M_n]) = \frac{1}{c_n} \mathbb{E} [cost]. \end{aligned} \quad (12)$$

Combining both Equations (10) and (12) concludes Theorem 3.

A.5 Proof of Theorem 4

Theorem 4. Let $(x_1, y_1), \dots, (x_T, y_T)$ be a sample stream, where $x_t \in \mathbb{R}^d$ and $y_t \in \{-1, +1\}$. Let T_B be the round that uses up the budgets, i.e., $B_{T_B+1} = B$. For any $\mu \in \mathbb{R}^d$, the expected mistakes of OA3 over budgets is bounded by:

$$\mathbb{E} \left[\sum_{T_B+1}^T M_t \right] \leq \sum_{T_B+1}^T \left[\frac{\ell_t(\mu)}{\rho_{min}} + y_t x_t^\top \mu_{T_B+1} \right],$$

where μ_{T_B+1} is the predictive vector of model, trained by all the previous queried samples.

Proof A.5. When running out of budget, the sample sequence is from $(x_{T_B+1}, y_{T_B+1}), \dots, (x_T, y_T)$. Now, for any t after T_B , the predictive vector $\mu_{t+1} = \mu_t = \mu_{T_B+1}$. Combining this with the fact:

$$\ell_t(\mu) \geq \rho_t (1 - y_t x_t^\top \mu) \Leftrightarrow y_t x_t^\top \mu \geq 1 - \frac{1}{\rho_t} \ell_t(\mu),$$

we have:

$$\begin{aligned} M_t &\leq M_t \left[y_t x_t^\top \mu_{T_B+1} + \frac{\ell_t(\mu)}{\rho_t} \right] \\ &\leq y_t x_t^\top \mu_{T_B+1} + \frac{\ell_t(\mu)}{\rho_{min}}, \end{aligned}$$

where we use $M_t \leq 1$. Then, we obtain:

$$\mathbb{E} \left[\sum_{T_B+1}^T M_t \right] \leq \sum_{T_B+1}^T \left[\frac{\ell_t(\mu)}{\rho_{min}} + y_t x_t^\top \mu_{T_B+1} \right],$$

which concludes Theorem 4.

A.6 Proof of Theorem 5

Theorem 5. Under the same condition in Theorem 4, by setting $\rho = \frac{\alpha_p T_n}{\alpha_n T_p}$, the sum performance of OA3 over budgets satisfies for any $\mu \in \mathbb{R}^d$:

$$\mathbb{E}[\text{sum}] \geq 1 - \frac{\alpha_n \rho_{max}}{T_n} \sum_{T_B+1}^T \left[\frac{\ell_t(\mu)}{\rho_{min}} + y_t x_t^\top \mu_{T_B+1} \right].$$

Proof A.6. From Theorem 4, we have:

$$\mathbb{E} \left[\sum_{\substack{T_B+1 \\ y_t=+1}}^T \rho M_t \right] \leq \sum_{\substack{T_B+1 \\ y_t=+1}}^T \rho \left[\ell_t(\mu) + y_t x_t^\top \mu_{T_B+1} \right], \quad (13)$$

$$\mathbb{E} \left[\sum_{\substack{T_B+1 \\ y_t=-1}}^T M_t \right] \leq \sum_{\substack{T_B+1 \\ y_t=-1}}^T \left[\ell_t(\mu) + y_t x_t^\top \mu_{T_B+1} \right]. \quad (14)$$

According to Equations (11), (13) and (14), we have:

$$\begin{aligned} \mathbb{E}[\text{sum}] &\geq 1 - \frac{\alpha_n}{T_n} \times \max\{1, \rho\} \sum_{T_B+1}^T \left[\frac{\ell_t(\mu)}{\rho_{min}} + y_t x_t^\top \mu_{T_B+1} \right] \\ &\geq 1 - \frac{\alpha_n \rho_{max}}{T_n} \sum_{T_B+1}^T \left[\frac{\ell_t(\mu)}{\rho_{min}} + y_t x_t^\top \mu_{T_B+1} \right], \end{aligned}$$

which concludes Theorem 5.

A.7 Proof of Theorem 6

Theorem 6. Under the same condition in Theorem 4, by setting $\rho = \frac{c_p}{c_n}$, the misclassification cost of OA3 over budgets satisfies for any $\mu \in \mathbb{R}^d$:

$$\mathbb{E}[\text{cost}] \leq c_n \rho_{max} \sum_{T_B+1}^T \left[\frac{\ell_t(\mu)}{\rho_{min}} + y_t x_t^\top \mu_{T_B+1} \right].$$

Proof A.7. Based on Equations (12), (13) and (14), we have:

$$\begin{aligned} \mathbb{E}[\text{cost}] &\leq c_n \max\{1, \rho\} \sum_{T_B+1}^T \left[\frac{\ell_t(\mu)}{\rho_{min}} + y_t x_t^\top \mu_{T_B+1} \right] \\ &\leq c_n \rho_{max} \sum_{T_B+1}^T \left[\frac{\ell_t(\mu)}{\rho_{min}} + y_t x_t^\top \mu_{T_B+1} \right], \end{aligned}$$

which concludes Theorem 6.

SECTION B ALGORITHMS

B.1 Diagonal Version of OA3

In this subsection, we provide details for diagonal version of OA3 (named, OA3_{diag}).

The difference between OA3 and OA3_{diag} is the update strategy. OA3_{diag} only exploits the diagonal elements of covariance when updating both the covariance matrix Σ and predictive vector μ . In other words, OA3_{diag} only considers the model confidence of each feature independently and ignores the correlations among different features. As a result, it can achieve faster computational efficiency than OA3.

Note that the initialization of Σ_1^{diag} is a identity matrix. All non-diagonal elements equal to 0. At round t , we only update diagonal elements of covariance matrix. To this end, we adjust the update rule

$$\Sigma_{t+1} = \Sigma_t - \frac{\Sigma_t x_t x_t^\top \Sigma_t}{\gamma + x_t^\top \Sigma_t x_t} \quad (15)$$

to

$$\Sigma_{t+1}^{diag} = \Sigma_t^{diag} - \frac{\Sigma_t^{diag} \circ x_t \circ \Sigma_t^{diag} \circ x_t}{\gamma + x_t \circ \Sigma_t^{diag} \circ x_t}, \quad (16)$$

where \circ is the element-wise product so that $\Sigma_{t+1}^{diag} \in \mathbb{R}^d$ can keep the diagonal property. Then, the diagonal update of μ_t is as follows:

$$\mu_{t+1} = \mu_t - \eta \Sigma_{t+1} \circ g_t. \quad (17)$$

We summarize the diagonal OA3 update strategy in Algorithm 1.

Algorithm 1 Diagonal Adaptive Asymmetric Update Strategy: **DiagUpdate**($\mu_t, \Sigma_t; x_t, y_t$).

Input $\rho = \frac{\alpha_p T_n}{\alpha_n T_p}$ for “sum” or $\rho = \frac{c_p}{c_n}$ for “cost”;

- 1: Receive a sample (x_t, y_t) ;
 - 2: Compute the loss $\ell_t(\mu_t)$, based on Equation (4);
 - 3: **if** $\ell_t(\mu_t) > 0$ **then**
 - 4: $\Sigma_{t+1}^{diag} = \Sigma_t^{diag} - \frac{\Sigma_t^{diag} \circ x_t \circ \Sigma_t^{diag} \circ x_t}{\gamma + x_t^\top \circ \Sigma_t^{diag} \circ x_t}$;
 - 5: $\mu_{t+1} = \mu_t - \eta \Sigma_{t+1} \circ g_t$, where $g_t = \partial \ell_t(\mu_t)$.
 - 6: **else**
 - 7: $\mu_{t+1} = \mu_t, \Sigma_{t+1}^{diag} = \Sigma_t^{diag}$.
 - 8: **end if**
 - 9: **Return** $\mu_{t+1}, \Sigma_{t+1}^{diag}$.
-

B.2 Sparse Sketch Algorithms

This section provides algorithms (Algorithm 2, 3 and 4) for Section 4.2.

Algorithm 2 Sparse Sketched Asymmetric Query Strategy: **SparseSketchQuery**(p_t).

Input $\rho_{max} = \max\{1, \rho\}$; query bias (δ_+, δ_-) for positive and negative predictions.

- 1: Variance $v_t = x_t^\top (I_d - U_{t-1}^\top F_{t-1}^\top (t-1) \Lambda_{t-1} H_{t-1} F_{t-1} U_{t-1}) x_t$;
 - 2: Compute the query parameter $q_t = |p_t| - \frac{1}{2} \frac{\eta \rho_{max}}{v_t + \gamma}$;
 - 3: **if** $q_t \leq 0$ **then**
 - 4: Set $q_t = 0$;
 - 5: **end if**
 - 6: **if** $p_t \geq 0$ **then**
 - 7: $p_t^+ = \frac{\delta_+}{\delta_+ + q_t}$;
 - 8: Draw a Bernoulli variable $Z_t \in \{0, 1\}$ with p_t^+ .
 - 9: **else**
 - 10: $p_t^- = \frac{\delta_-}{\delta_- + q_t}$;
 - 11: Draw a Bernoulli variable $Z_t \in \{0, 1\}$ with p_t^- .
 - 12: **end if**
 - 13: **Return** Z_t .
-

Algorithm 3 Sparse Oja's Sketch for OA3**Input** m, \hat{x} and stepsize matrix Γ_t .**Internal State** t, Λ, F, U, K and H .**SparseSketchInit**(m)

- 1: Set $t = 0, F = K = H = I_m, \Lambda = 0_{m \times m}$ and U to any $m \times d$ matrix with orthonormal rows;
- 2: Return (Λ, F, U, H) .

SparseSketchUpdate(\hat{x})

- 1: Update $t \leftarrow t + 1$;
- 2: $\Lambda = (I_m - \Gamma_t)\Lambda + \Gamma_t \text{diag}\{FU\hat{x}\}^2$;
- 3: Set $\delta = F^{-1}\Gamma_t FU\hat{x}^\top$;
- 4: $K \leftarrow K + U\hat{x}\delta^\top + \delta\hat{x}^\top U^\top + \delta\hat{x}^\top \hat{x}\delta^\top$;
- 5: $U \leftarrow U + \delta\hat{x}^\top$;
- 6: $(L, Q) \leftarrow \text{Decompose}(F, K)$,
where $LQU = FU$ and QU is orthogonal;
- 7: Set $F = Q$;
- 8: Set $H = \text{diag}\{\frac{1}{1+t\Lambda_{1,1}}, \dots, \frac{1}{1+t\Lambda_{m,m}}\}$;
- 9: Return $(\Lambda, F, U, H, \delta)$.

Algorithm 4 Decompose(F, K)**Input** $F \in \mathbb{R}^{m \times m}$ and Gram matrix $K = UU^\top \in \mathbb{R}^{m \times m}$;**Initialization** $L = 0_{m \times m}$ and $Q = 0_{m \times m}$;

- 1: **for** $i = 1 \rightarrow m$ **do**
- 2: Let f^\top be the i -th row of F ;
- 3: Compute $\alpha = QKf, \beta = f - Q^\top\alpha$ and $c = \sqrt{\beta^\top K\beta}$;
- 4: **if** $c \neq 0$ **then**
- 5: Insert $\frac{1}{c}\beta^\top$ to the i -th row of Q ;
- 6: **end if**
- 7: Set the i -th entry of α to be c ;
- 8: Insert α to the i -th row of L ;
- 9: **end for**
- 10: Delete the all-zero columns of L and all-zero rows of Q ;
- 11: Return (L, Q) .

SECTION C**ADDITIONAL EXPERIMENTS**

This section provides the additional experimental results.

C.1 Cost Evaluation of Query Biases

This subsection evaluates the influence of the query biases on *cost* results under fixed budgets, where both query biases (δ_+ and δ_-) are selected from $[10^{-5}, \dots, 10^5]$, and other parameters are fixed. From Fig. 1, we draw several observations.

First, the best results (*i.e.*, deep blue) are usually achieved when $\delta_+ \in \{10, 10^2, 10^3, 10^4\}$ and $\delta_- \in \{1, 10\}$. This observation suggests the potential settings of query biases.

Second, when both δ_+ and δ_- are large (*i.e.*, the upper right corner), OA3 obtains relatively good performance; while when both δ_+ and δ_- are small (*i.e.*, the bottom left corner), OA3 performs relatively bad. This observation further validates the findings in *sum* results.

Finally, OA3 with large δ_+ and small δ_- (the upper left corner) outperforms the performance with large δ_- and small δ_+ (the bottom right corner). This means that OA3 performs better when querying more samples with

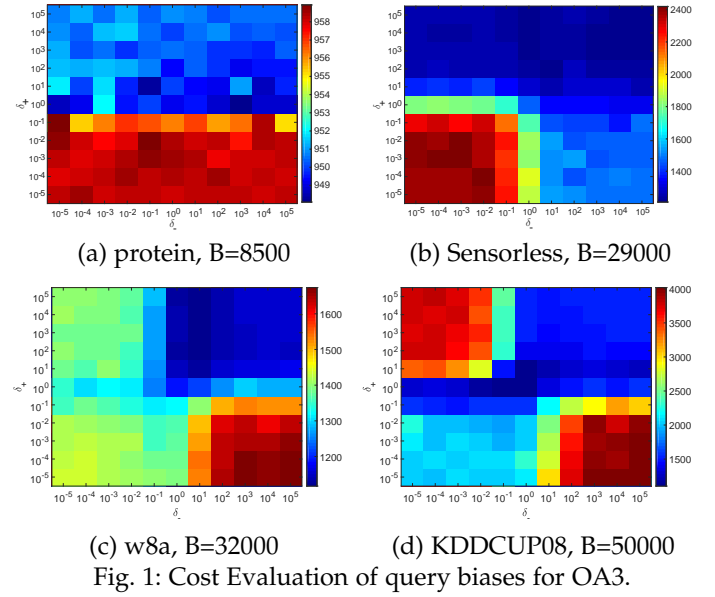


Fig. 1: Cost Evaluation of query biases for OA3.

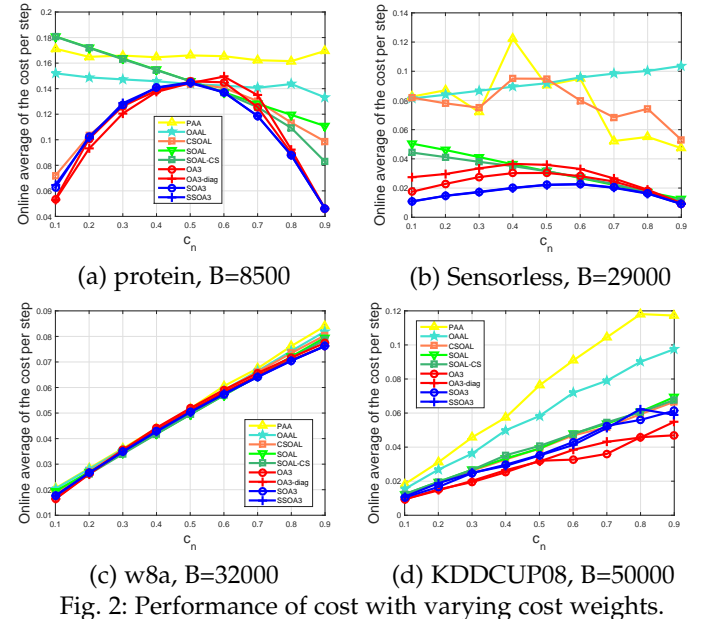


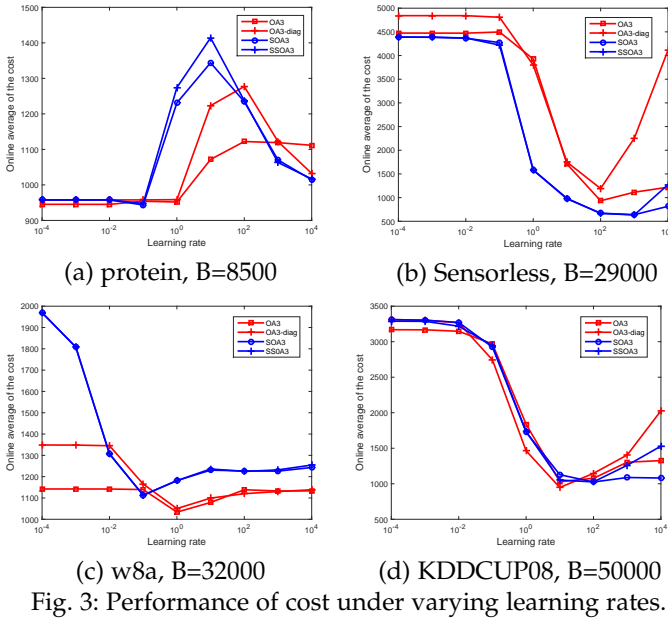
Fig. 2: Performance of cost with varying cost weights.

the positive prediction and training itself by more positive samples. The main reason is that the positive samples are often more important in real-world tasks. Thus, our algorithms would be more effective in practical tasks due to the good algorithm characteristics, compared with the algorithms that treat all data equally, or tend to query more negative data.

C.2 Cost Evaluation of Cost Weights

In this subsection, we evaluate the influence of different cost weights on the *cost* metric, *i.e.*, c_n , where $c_p = 1 - c_n$. Fig. 2 summarize the results of *cost* metric under fixed budgets.

From the results, we find our proposed algorithms consistently outperform all other algorithms with different weights. This observation shows that OA3 based algorithms have a wide selection range of cost weights, which further validates the effectiveness of our proposed methods again.



C.3 Cost Evaluation of Learning Rate

In this subsection, we evaluate the influence of learning rate in terms of the *cost* performances. We examine proposed methods with different learning rates η from $[10^{-4}, 10^{-3}, \dots, 10^3, 10^4]$.

From Fig. 3, results show the suitable range of learning rates for different datasets. We find OA3 algorithms achieve the best result on most cost datasets. Moreover, SOA3 and SSOA3 can achieve a relatively good performance on most datasets, and sometimes even better, compared with OA3, which also confirms that the sketched versions of OA3 are good choices to balance the performance and efficiency.

C.4 Evaluation of Regularized Parameter

In previous experiments, the regularization parameter is set to 1 (*i.e.*, $\gamma=1$) by default. However, the rationality of this default setting has not been verified. In this subsection, we examine the performance of our algorithms with different regularization parameters γ from $[10^{-4}, 10^{-3}, \dots, 10^3, 10^4]$.

From Fig. 4 and 5, we find the optimal selection of γ depends on datasets and methods. Nevertheless, in most cases, the setting $\gamma=1$ achieves the best or fairly good performance. This observation validates the practical value of our algorithms with the default setting in real-world datasets.

C.5 Evaluation of Query Strategies

In this subsection, we examine our asymmetric query strategy. We compare OA3 with two variants of OA3 with weak query rules: (1) OA3 with the “First come first served” strategy (OA3-F), which is the pure updating version without query strategies; (2) OA3 with the random query strategy (OA3-R).

From the results in Fig. 6 and 7, our asymmetric query strategy outperforms both OA3-R and OA3-F on most datasets, which verifies the effectiveness of our query strategy. Besides, when the number of samples is small, the performance of OA3 and OA3-F are almost same on most

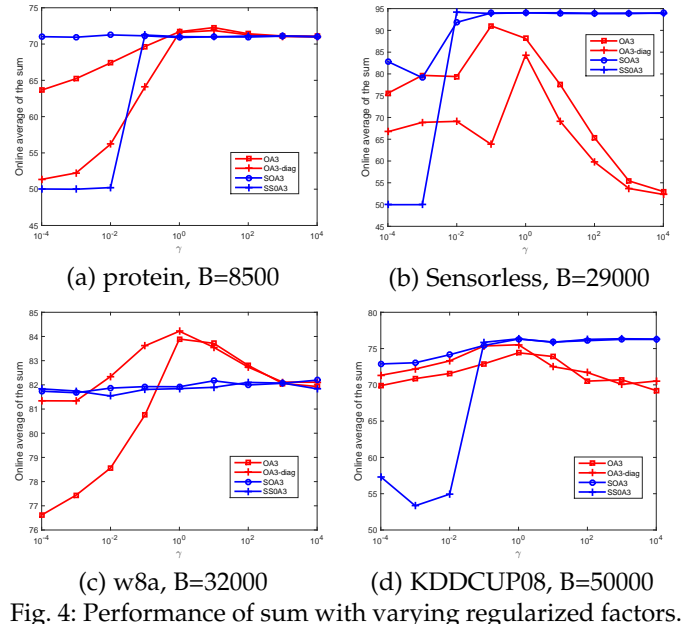


Fig. 4: Performance of sum with varying regularized factors.

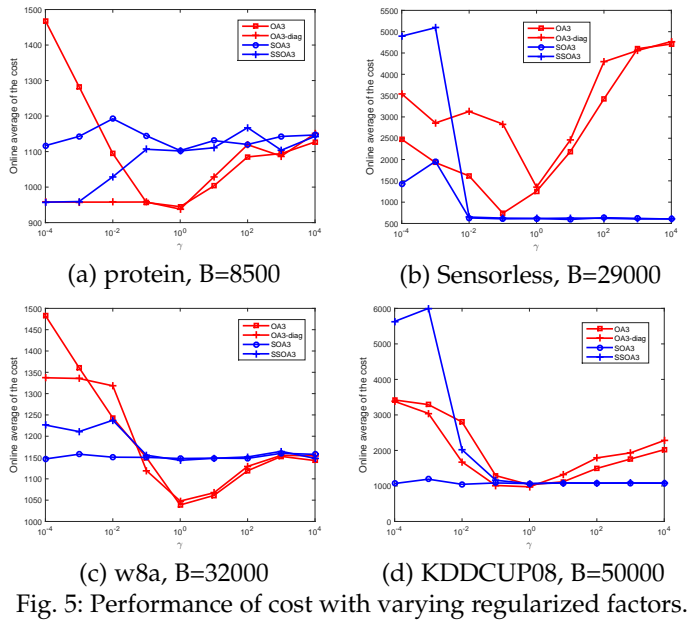


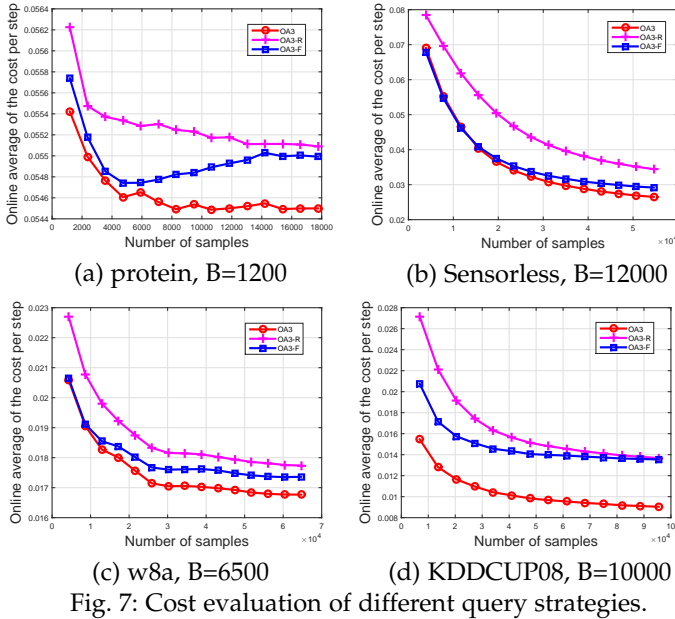
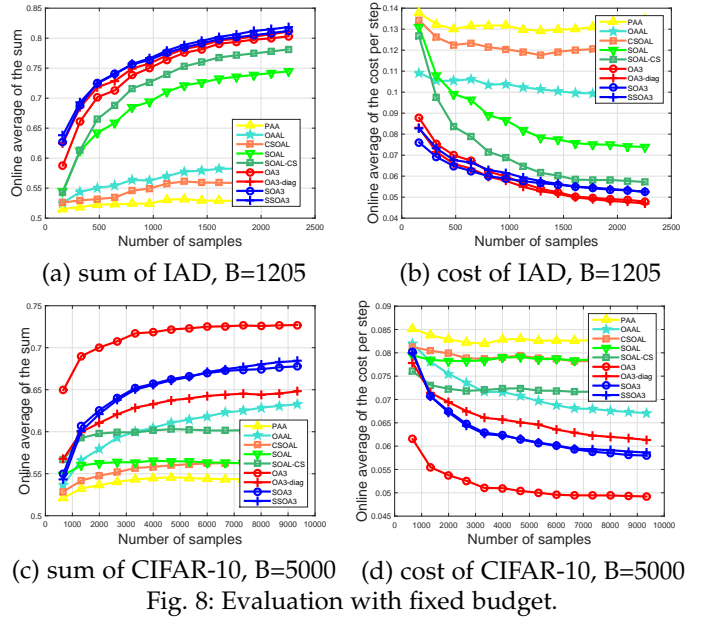
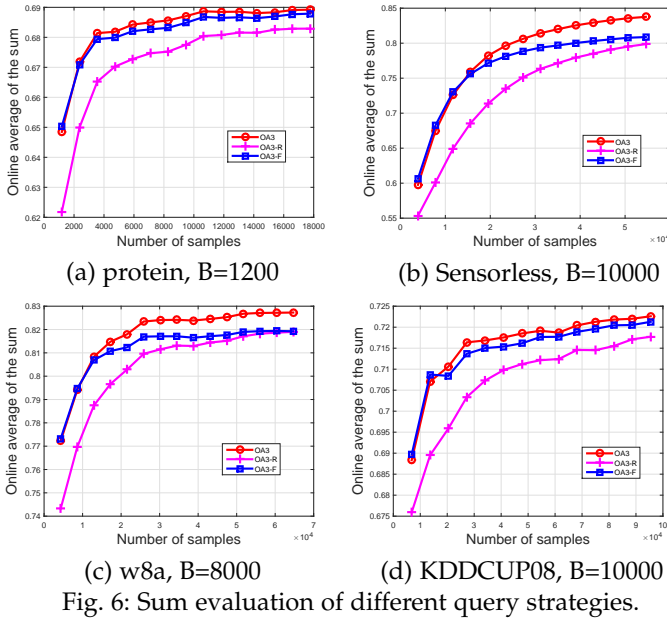
Fig. 5: Performance of cost with varying regularized factors.

datasets. One possible reason is that at the beginning of online learning, each sample is informative and thus is queried by OA3. In this case, OA3 is nearly same to OA3-F. Note that our query strategy also has theoretical guarantees which we described in Section A.

C.6 Evaluation on High Dimensional Datasets

In the main text, we have reported the results of *sum* metric on the two higher dimensional datasets. In this subsection, we present the results of *cost* metric and provide more discussions. Table 1 summarizes the statistics of the datasets. Fig. 8 shows the development of *sum* and *cost* performance. Table 2 provides more details in terms of *cost* metric.

From the empirical results, OA3 outperforms all first-order algorithms (PAA, OAAL and CSOAL) and other second-order algorithms (*i.e.*, SOAL and SOAL-CS). However, the computation cost of all second-order methods (*i.e.*, OA3, SOAL and SOAL-CS) is a huge problem when the



by adding the misclassified sample with a constant weight. Recently, many margin-based methods [3], [4] emerged, and show good performance. Despite their superiority, these methods only adopt samples' first-order information, which may result in slow convergence rate. To eliminate this limitation, many second-order methods [5], [6], [9], [10] were proposed, and significantly improve the performance with faster convergence.

Active learning aims to train a well-performed model by querying the labels of a small subset of informative data. It helps to reduce the labeling cost and attracts wide attention [11], [13], [14], [15], [16]. Particularly, one classic work [15] proposes a sampling method by drawing a Bernoulli random variable, which has been validated as effective and inspires many studies [17], [18]. Despite the effectiveness, most active algorithms [19], [20], [21], [23] assume that all the data are provided in advance, which is impractical in real-world problems. To address this limitation, OAL has emerged and raised wide research interest [24], [25], [26], [27].

dimension of data increases. In contrast, our proposed SOA3 and SSOA3 demonstrate better trade-off between efficiency and performance than OA3. It worth mentioning that, from Table 3, our SOA3 and SSOA3 show larger speedup ratios when the dimensionality increase, which further verify the efficiency of the proposed methods.

TABLE 1: Statistics of two high-dimensional datasets

Dataset	#Examples	#Features	#Pos:#Neg
IAD	2410	1558	1:4.9
CIFAR-10	10000	3072	1:9.0

SECTION D RELATED WORK

Online learning has been a hot research topic in machine learning for many years. One pioneering method is Perceptron algorithm [2], which updates the predictive vector

Although OAL has been studied widely, only a few studies focus on class-imbalanced issues. One classic method is CSOAL [18], which adopts a cost-sensitive update rule to solve imbalance problems. Another famous method is OAAL [17], which uses an asymmetric query rule to handle imbalanced data. However, both pioneering methods only consider the asymmetric strategy from one isolated perspective, which restricts their abilities in imbalance problems. Moreover, both methods only consider first-order information of samples, which limits their performance. To address these limitations, we exploit samples' second-order information and develop a new asymmetric strategy, considering both optimization and label queries, to handle imbalance problems and accelerate convergence rate.

Then, we highlight several differences of OA3 with several conceptually related methods, *i.e.* [23], [26]. In [23], a cost overlapped active learning algorithm is proposed to study the cost problem, but it is not an online method and does not consider class-imbalance issues. A second-

TABLE 2: Cost evaluation on high-dimensional datasets

Algorithm	"cost" on CIFAR-10				"cost" on IAD			
	Cost	Sensitivity(%)	Specificity (%)	Time(s)	Cost	Sensitivity(%)	Specificity (%)	Time(s)
PAA	830.720 ± 34.970	17.313 ± 15.064	90.793 ± 15.308	0.516	325.320 ± 39.882	19.289 ± 19.460	85.539 ± 16.220	0.064
OAAAL	664.890 ± 15.590	58.766 ± 1.571	67.545 ± 0.997	0.472	241.620 ± 7.927	53.333 ± 2.513	64.905 ± 1.858	0.062
CSOAL	778.650 ± 58.513	21.124 ± 9.960	92.749 ± 3.781	0.463	301.160 ± 48.723	23.088 ± 14.965	90.639 ± 5.080	0.058
SOAL	790.440 ± 12.342	18.478 ± 1.908	94.100 ± 0.786	505.121	178.790 ± 38.081	53.554 ± 10.719	95.884 ± 1.130	21.788
SOAL-CS	719.380 ± 18.485	27.920 ± 2.729	92.505 ± 0.861	556.762	138.270 ± 6.059	68.235 ± 1.835	89.196 ± 1.654	28.812
OA3	489.540 ± 9.696	79.791 ± 3.050	65.898 ± 3.636	1859.225	114.680 ± 8.430	85.270 ± 3.898	69.735 ± 5.624	45.005
OA3 _{diag}	607.460 ± 39.401	62.169 ± 10.385	70.508 ± 6.869	105.221	111.580 ± 8.055	84.118 ± 3.506	73.397 ± 5.555	6.609
SOA3	576.430 ± 27.359	71.433 ± 8.647	64.643 ± 8.730	66.108	125.480 ± 8.543	97.745 ± 1.032	41.459 ± 4.996	4.409
SSOA3	582.720 ± 49.878	72.328 ± 8.699	63.043 ± 10.479	50.397	125.160 ± 19.941	93.627 ± 6.757	49.171 ± 20.764	3.177

TABLE 3: Speedup ratios of sketched algorithms on different datasets

Time (s)	Sensorless, $d=48$	KDDCUP08, $d=117$	w8a, $d=300$	protein, $d=357$	IAD, $d=1558$	CIFAR-10, $d=3072$
OA3	0.966	7.066	14.118	12.511	44.674	1948.292
SOA3	0.862 (×1.12)	3.779 (×1.87)	4.556 (×3.10)	1.395 (×8.97)	4.084 (×10.94)	66.739 (×29.19)
SSOA3	0.920 (×1.05)	3.376 (×2.09)	3.398 (×4.15)	1.004 (×12.46)	3.215 (×13.90)	52.126 (×37.38)

order online active learning algorithm (SOAL) is proposed in [26]. This method adopts second-order information, but it ignores the budget limitations and class-imbalance problems. A cost-sensitive version of SOAL is presented in [26]. This method considers the asymmetric losses, but it lacks theoretical guarantees, and ignores budget limitations and asymmetric query strategies.

Finally, sketching methods are a good choice to balance the performance and efficiency of OA3 algorithms. A well-known family of methods for sketching is the Random Projection [28], [29], [30], [31], [32], [33], which relies on the properties of random low dimensional subspaces and strong concentration of measure phenomena. However, the theoretical guarantees of the Random Projection may perform terrible when the rank of approximated matrix is near full-rank [35]. To address the above issue, researchers recently proposed the Frequent Direction Sketch [36], [37], which is a class of deterministic methods that derives from the similarity comparison between matrix sketching problem and item frequency estimation problem. For the Frequent Direction Sketch methods, the regret bound depends on a super-parameter and a square root term, which are not controlled by the sketching algorithms [35]. To better focus on the dominant part of the spectrum for deterministic sketching, an Ojas sketch algorithm was recently proposed [35] based on Ojas algorithm [38], [39].

A brief version of this paper had been published in SIGKDD conference [40]. Compared with it, this journal manuscript makes several significant extensions, including (1) two updated variants with sketching methods, and some theoretical analyses about their time complexity; (2) more empirical studies to evaluate the proposed algorithms.

REFERENCES

- [1] Y. Zhang, P. Zhao, S. Niu, Q. Wu, J. Cao, J. Huang, M. Tan. Online adaptive asymmetric active learning for limited budgets. *IEEE Transactions on Knowledge and Data Engineering*, 2019.
- [2] Y. Freund, R. E. Schapire. Large margin classification using the perceptron algorithm. *Machine learning*, 1999, Vol. 37, pp. 277-296.
- [3] K. Crammer, O. Dekel, J. Keshet, S. Shalev-Shwartz, Y. Singer. Online passive-aggressive algorithms. *Journal of Machine Learning Research*, 2006, pp. 551-585.
- [4] J. Wang, P. Zhao and S. C. Hoi. Cost-sensitive online classification. *IEEE Transactions on Knowledge and Data Engineering*, 2014, vol. 26, no. 10, pp. 2425-2438.
- [5] K. Crammer, A. Kulesza, M. Dredze. Adaptive regularization of weight vectors. In *Advances in Neural Information Processing Systems*, 2009, pp. 414-422.
- [6] P. Zhao, F. Zhuang, M. Wu, X. Li, S. C. H. Hoi. Cost-sensitive online classification with adaptive regularization and its applications. *IEEE International Conference on Data Mining*, 2015, pp. 649-658.
- [7] J. Cao, L. Mo, Y. Zhang, K. Jia, C. Shen, M. Tan. Multi-marginal Wasserstein GAN, In *Advances in Neural Information Processing Systems*, 2019.
- [8] Y. Zhang, Y. Wei, P. Zhao, S. Niu, Q. Wu, M. Tan, J. Huang. Collaborative unsupervised domain adaptation for medical image diagnosis, In *Medical Imaging meets NeurIPS*, 2019.
- [9] N. Cesa-Bianchi, A. Conconi, C. Gentile. A second-order perceptron algorithm. *SIAM Journal on Computing*, 2005, No. 3, pp. 640-668.
- [10] P. Zhao, Y. Zhang, M. Wu, S. C. Hoi, M. Tan, J. Huang. Adaptive cost-sensitive online classification. *IEEE Transactions on Knowledge and Data Engineering*, 2018.
- [11] C. Aggarwal, X. Kong, Q. Gu, J. Han, P. Yu. Active learning: a survey, *Data Classification: Algorithms and Applications*, 2014.
- [12] Y. Guo, Y. Zheng, M. Tan, Q. Chen, J. Chen, P. Zhao, J. Huang. NAT: Neural architecture transformer for accurate and compact architectures. *Advances in Neural Information Processing Systems*, 2019.
- [13] K. Fujii, H. Kashima. Budgeted stream-based active learning via adaptive submodular maximization. In *Advances in Neural Information Processing Systems*, 2016, pp. 514-522.
- [14] V. S. Sheng, F. Provost, P. G. Ipeirotis. Get another label? improving data quality and data mining using multiple, noisy labelers. In *ACM SIGKDD International Conference on Knowledge Discovery and Data Mining*, 2008, pp. 614-622.
- [15] N. Cesa-Bianchi, C. Gentile, L. Zaniboni. Worst-case analysis of selective sampling for linear classification. *Journal of Machine Learning Research*, 2006, No. 7, pp. 1205-1230.
- [16] M. Fang, X. Zhu, B. Li, W. Ding, X. Wu. Self-taught active learning from crowds. In *IEEE International Conference on Data Mining*, 2012, pp. 858-863.
- [17] X. Zhang, T. Yang, P. Srinivasan. Online asymmetric active learning with imbalanced data. In *ACM SIGKDD International Conference on Knowledge Discovery and Data Mining*, 2016, pp. 2055-2064.
- [18] P. Zhao, S. C. Hoi. Cost-sensitive online active learning with application to malicious URL detection. In *ACM SIGKDD International Conference on Knowledge Discovery and Data Mining*, 2013, pp. 919-927.

- [19] N. Abe, B. Zadrozny, J. Langford. Outlier detection by active learning. In *ACM SIGKDD International Conference on Knowledge Discovery and Data Mining*, 2006, pp. 504-509.
- [20] S. Chakraborty, V. Balasubramanian, A. Sankar, S. Panchanathan, J. Ye. Batchrank: A novel batch mode active learning framework for hierarchical classification. In *ACM SIGKDD International Conference on Knowledge Discovery and Data Mining*, 2015, pp. 99-108.
- [21] S. J. Huang, J. L. Chen, X. Mu, Z. H. Zhou. Cost-Effective active learning from diverse labelers. In *International Joint Conference on Artificial Intelligence*, 2017, pp. 1879-1885.
- [22] Y. Zhang, H. Chen, Y. Wei, P. Zhao, J. Cao, X. Fan, X. Lou, H. Liu, X. Han, j. Yao, Q. Wu, M. Tan, J. Huang. From whole slide imaging to microscopy: Deep microscopy adaptation network for histopathology cancer image classification. In *International Conference on Medical Image Computing and Computer-Assisted Intervention*, 2019, pp. 360-368.
- [23] A. Krishnamurthy, A. Agarwal, T. Huang, D. Hal, J. Langford. Active learning for cost-sensitive classification. In *International Conference on Machine Learning*, 2017, pp. 1915-1924.
- [24] J. Lu, P. Zhao, S. C. Hoi. Online passive-aggressive active learning. *Machine Learning*, 2016, Vol. 103, No. 2, pp. 141-183.
- [25] I. Zliobaite, A. Bifet, B. Pfahringer, G. Holmes. Active learning with drifting streaming data. *IEEE Transactions on Neural Networks and Learning Systems*, 2014, Vol. 25, No. 1, pp. 27-39.
- [26] S. Hao, J. Lu, P. Zhao, C. Zhang, S. C. Hoi, C. Miao. Second-order online active learning and its applications. *IEEE Transactions on Knowledge and Data Engineering*, 2017.
- [27] Z. Ferdowsi, R. Ghani, R. Settmi. Online active learning with imbalanced classes. In *IEEE International Conference on Data Mining*. 2013, pp. 1043-1048.
- [28] S. S. Vempala. The random projection method. *American Mathematical Society*, 2004.
- [29] T. Sarlos. Improved approximation algorithms for large matrices via random projections. In *Annual Symposium on Foundations of Computer Science*, 2006, pp. 143-152.
- [30] E. Liberty, F. Woolfe, P. G. Martinsson, V. Rokhlin, M. Tygert. Randomized algorithms for the low-rank approximation of matrices. *Proceedings of the National Academy of Sciences*, 2007.
- [31] D. Achlioptas. Database-friendly random projections: Johnson-Lindenstrauss with binary coins. *Journal of Computer and System Sciences*, 2003, Vol. 66, No. 4, pp. 671-687.
- [32] P. Indyk, R. Motwani. Approximate nearest neighbors: towards removing the curse of dimensionality. In *Annual Symposium on Theory of Computing*, 1998, pp. 604-613.
- [33] D. M. Kane, J. Nelson. Sparsifier johnson-lindenstrauss transforms. *Journal of the ACM*, 2014, Vol. 61, No. 1, pp. 4.
- [34] Y. Zhang, G. Shu, Y. Li. Strategy-updating depending on local environment enhances cooperation in prisoners dilemma game. *Applied Mathematics and Computation*, 2017, vol. 301, pp. 224-232.
- [35] H. Luo, A. Agarwal, N Cesa-Bianchi. Efficient second order online learning by sketching. In *Advances in Neural Information Processing Systems*, 2016, pp. 902-910.
- [36] M. Ghashami, E. Liberty, J. M. Phillips, D. P. Woodruff. Frequent directions: Simple and deterministic matrix sketching. *SIAM Journal on Computing*, 2016, Vol. 45, No. 5, pp. 1762-1792.
- [37] E. Liberty. Simple and deterministic matrix sketching. *ACM International Conference on Knowledge Discovery and Data Mining*, 2013, pp. 581-588.
- [38] E. Oja. Simplified neuron model as a principal component analyzer. *Journal of Mathematical biology*, 1982, Vol. 15, No. 3, pp. 267-273.
- [39] E. Oja, J. Karhunen. On stochastic approximation of the eigenvectors and eigenvalues of the expectation of a random matrix. *Journal of Mathematical Analysis and Applications*, 1985, vol. 106, pp. 69-84.
- [40] Y. Zhang, P. Zhao, J. Cao, W. Ma, J. Huang, Q. Wu, M. Tan. Online adaptive asymmetric active learning for budgeted imbalanced data. In *ACM SIGKDD International Conference on Knowledge Discovery and Data Mining*, 2018, pp. 2768-2777.